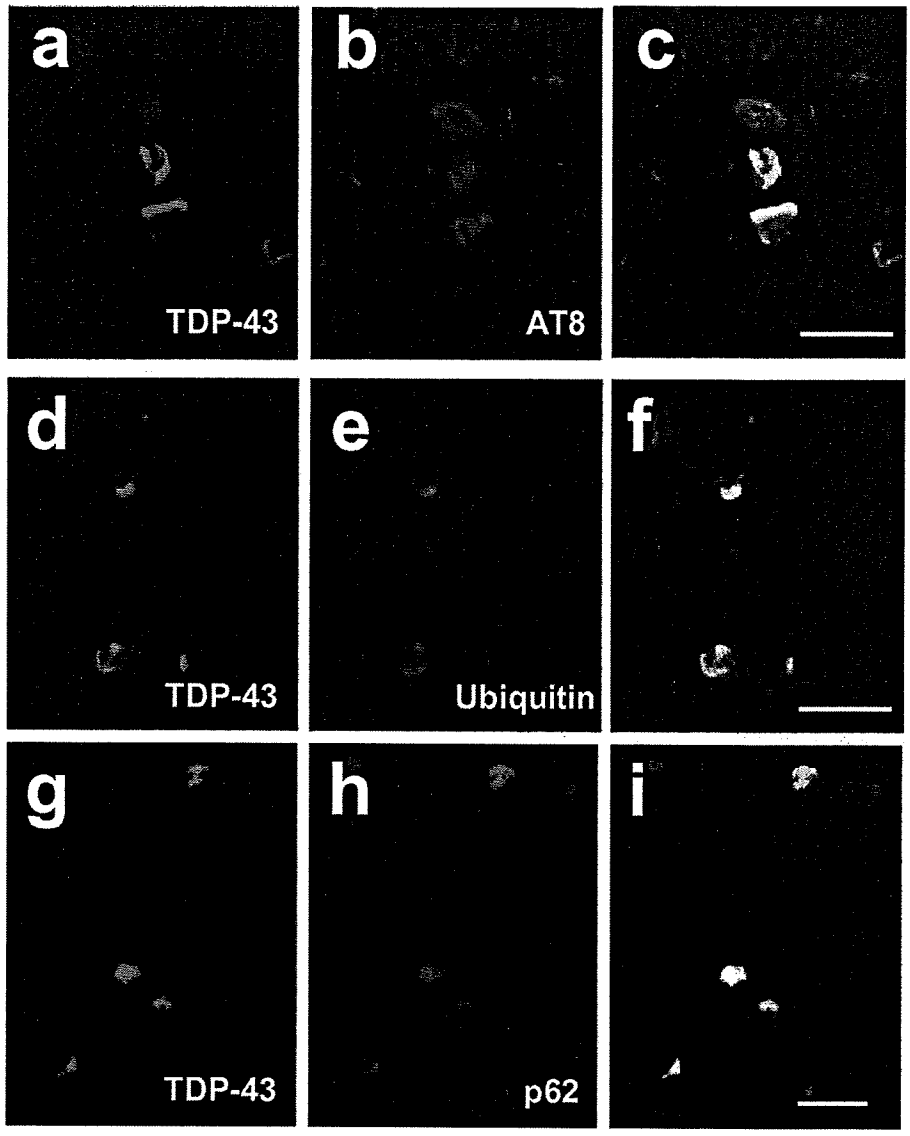

Fig. 4 Double-labeling for TAR-DNA-binding protein 43 (TDP-43) (a, d, g), phospho-tau (b), ubiquitin (e), and p62 (h) with merged images (c, f, i). Intracellular abnormal TDP-43 (a) accumulation is partially colocalized with phospho-tau (b), whereas TDP-43 (d, g) and ubiquitin (e) or p62 (h) show almost complete coexistence. Scale bars: 10 μm.

no deposition in the dentate gyrus.[16] They also showed, using a semi-quantative method, that in FTLD-U and FTLD with motor neuron disease (FTLD-MND) cases, TDP-43 deposited in the dentate gyrus at very high density.[16] Therefore, the rate and density of TDP-43 deposition in dentate granular cells of AD subjects might vary and be different from those of FTLD-U. This notion is supported by a very recent report describing AD cases that showed no TDP-43 deposition in the hippocampus but in the amygdala.[22]

Hu *et al.* have recently reported the region-specific distribution and density of TDP-43-positive neuronal cytoplasmic inclusions in AD and suggested a progression of TDP-43 pathology in AD, spreading from limbic structures in the medial temporal lobe to multimodal association cortices in the temporal lobes and then to other higher-order association cortices.[22] In their study, no case demonstrated abnormal TDP-43 immunoreactivity in the frontal cortex without showing the inclusions in the entorhinal cortex. However, as shown in Figure 2d, our topographical examination demonstrated that some cases might show a large amount of frontal TDP-43 pathology without occipitotemporal gyrus deposition. The temporal progression pattern of TDP-43 deposition in AD is a subject of curiosity and it is also important to understand the significance of this protein accumulation in the disease process.

Another interesting issue that our topographical study showed was the massive TDP-43 deposition in the frontal but not in the parietal and occipital cortices. Previous studies also showed the deposition in neocortical areas of AD; however, the density was not reported[14] or relatively low.[16,22] Yet our cases showed highly dense deposition in the frontal cortex. If we use the semi-quantitative criteria of Hu *et al.*, our cases showed class 3 deposition (multiple

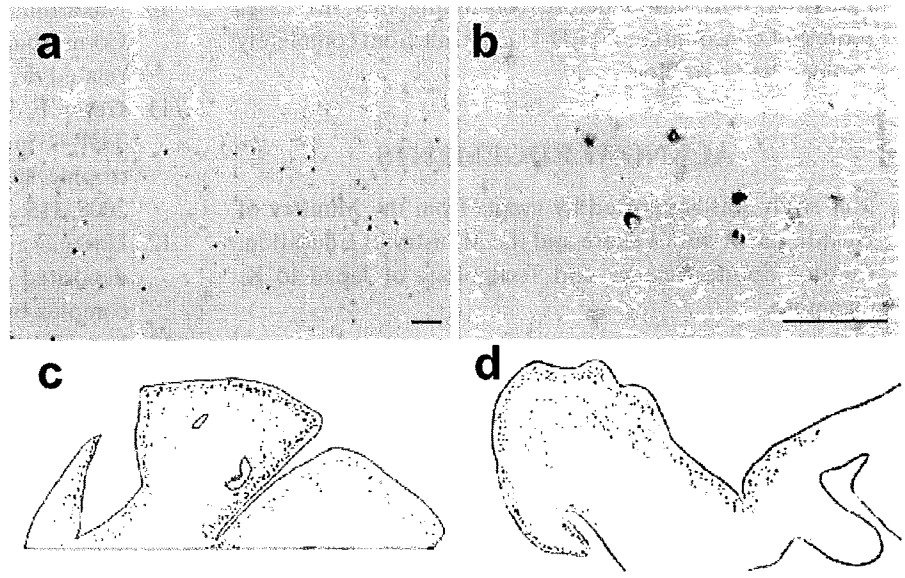

Fig. 5 Distribution of TAR-DNA-binding protein 43 (TDP-43)-positive inclusions in the frontal cortex. In the frontal cortex, abnormal TDP-43 immunoreactivity is distributed along cortical layers (a) depositing as intracellular inclusions (b). Widespread distribution of TDP-43-positive inclusions in two representative cases is shown in (c) and (d). Scale bars: a, 100 μm; b, 50 μm.

neuronal cytoplasmic inclusions (NCIs) identified in each 400× field) in the frontal cortex, whereas class 0.5 deposition (1–5 NCIs in the entire section) was the average in their study.[22] Higashi *et al.* also examined abnormal TDP-43 accumulation in neocortices.[16] Five of 15 AD cases showed TDP-43-positive inclusions in the hippocampal formation; however, immunoreactivity was not found in the superior frontal cortices. Thus, it is possible that emerging TDP-43-positive inclusions in the frontal cortex might be different between AD cases.

To obtain the detailed subcellular localization of TDP-43-positive inclusions, the sections were double-labeled with anti-TDP-43 and anti-phosphorylated tau antibodies. As previously reported, the partial colocalization of both proteins was evident, but its incidence rate was low.[14] Given the finding that neurofibrillary tangle distribution is independent from TDP-43 localization (Fig. 3a,c), TDP-43-positive inclusions and neurofibrillary tangles might be self-determining. Besides, almost no α-synuclein immunoreactivity was detected in the hippocampal area of five cases, suggesting that the deposition of TDP-43 and α-synuclein in AD might be independent phenomena. This notion is also supported by the results of Higashi *et al.* demonstrating only a few TDP-43-positive neuronal cytoplasmic inclusions within α-synuclein-positive cortical-type Lewy bodies in AD.[16]

Because accumulated TDP-43 was highly ubiquitinated, we also stained the sections with anti-p62 antibody. p62 is a stress-responsive protein containing a ubiquitin-associated domain in the C-termini.[23,24] p62 has been observed in ubiquitin-containing intraneuronal or intraglial inclusions such as neurofibrillary tangles,[25] Pick bodies, Lewy bodies, glial cytoplasmic inclusions in multiple system atrophy,[26] and skein-like and basophilic inclusions in ALS.[27] As expected, TDP-43-positive inclusions were well colocalized with the p62 protein (97.5%). This is the first report showing that neuronal TDP-43-positive inclusions in AD are p62-positive. In FTLD-U, TDP-43-trapped inclusions in the gray matter are ubiquitinated[1] and numerous p62-positive inclusions were detected there.[28] However, in white matter of FTLD-MND brains, abnormal TDP-43-positive inclusions were colocalized with p62, but not with ubiquitin.[29] Thus, it might be possible to speculate that TDP-43 depositions in neurons in the gray matter and glia in the white matter might take place in different ways,[29] and in this sense, a mechanism causing neuronal TDP-43-positive inclusions in AD might be similar to that leading to FTLD-U cortical pathology.

In the initial report demonstrating the TDP-43 pathology of AD, Amador-Ortiz *et al.* described the morphological and biochemical similarities of TDP-43 deposition both in AD and FTLD-U, and indicated that these cases might represent a combined disease, that is, mixed AD/FTLD-U.[14] However, Higashi *et al.* claimed that the neuroanatomical distribution of TDP-43-positive inclusions in AD was clearly different from that in FTLD-U cases.[16] In their cases, the amygdala and hippocampus demonstrated more severe TDP-43 pathology in AD than in FTLD-U. Moreover, in the frontal cortex and basal ganglia that are vulnerable to TDP-43 pathology in FTLD-U, TDP-43 pathology was not observed in their AD cases. On the basis of these findings, they suggested that FTLD-U might have a proximate pathogenic mechanism leading to TDP-43 aggregation that is different from that of AD. However, our cases demonstrating numerous frontal TDP-43 depositions apparently showed that their findings are not always the case in AD. Thus, we consider that the accumulation of AD cases and age-matched control studies showing TDP-43

pathology is required before concluding that the cases represent concomitant FTLD-U or result from completely independent pathology.

ACKNOWLEDGEMENTS

This study was supported by grants from the Ministry of Health, Labor and Welfare and the Ministry of Education, Culture, Sports, Science and Technology of Japan to K. Okamoto.

REFERENCES

1. Neumann M, Sampathu DM, Kwong LK *et al.* Ubiquitinated TDP-43 in frontotemporal lobar degeneration and amyotrophic lateral sclerosis. *Science* 2006; **314**: 130–133.
2. Neumann M, Kwong LK, Sampathu DM, Trojanowski JQ, Lee VM. TDP-43 Proteinopathy in frontotemporal lobar degeneration and amyotrophic lateral sclerosis: protein misfolding diseases without amyloidosis. *Arch Neurol* 2007; **64**: 1388–1394.
3. Kwong LK, Neumann M, Sampathu DM, Lee VM, Trojanowski JQ. TDP-43 proteinopathy: the neuropathology underlying major forms of sporadic and familial frontotemporal lobar degeneration and motor neuron disease. *Acta Neuropathol* 2007; **114**: 63–70.
4. Cairns NJ, Neumann M, Bigio EH *et al.* TDP-43 in familial and sporadic frontotemporal lobar degeneration with ubiquitin inclusions. *Am J Pathol* 2007; **171**: 227–240.
5. Mackenzie IR, Bigio EH, Ince PG *et al.* Pathological TDP-43 distinguishes sporadic amyotrophic lateral sclerosis from amyotrophic lateral sclerosis with SOD1 mutations. *Ann Neurol* 2007; **61**: 427–434.
6. Tan CF, Eguchi H, Tagawa A *et al.* TDP-43 immunoreactivity in neuronal inclusions in familial amyotrophic lateral sclerosis with or without SOD1 gene mutation. *Acta Neuropathol* 2007; **113**: 535–542.
7. Davidson Y, Kelley T, Mackenzie IR *et al.* Ubiquitinated pathological lesions in frontotemporal lobar degeneration contain the TAR DNA-binding protein, TDP-43. *Acta Neuropathol* 2007; **113**: 521–533.
8. Kwong LK, Neumann M, Sampathu DM, Lee VM, Trojanowski JQ. TDP-43 proteinopathy: the neuropathology underlying major forms of sporadic and familial frontotemporal lobar degeneration and motor neuron disease. *Acta Neuropathol* 2007; **114**: 63–70.
9. Arai T, Hasegawa M, Akiyama H *et al.* TDP-43 is a component of ubiquitin-positive tau-negative inclusions in frontotemporal lobar degeneration and amyotrophic lateral sclerosis. *Biochem Biophys Res Commun* 2006; **351**: 602–611.
10. Nakashima-Yasuda H, Uryu K, Robinson J *et al.* Co-morbidity of TDP-43 proteinopathy in Lewy body related diseases. *Acta Neuropathol* 2007; **114**: 221–229.
11. Geser F, Winton MJ, Kwong LK *et al.* Pathological TDP-43 in parkinsonism-dementia complex and amyotrophic lateral sclerosis of Guam. *Acta Neuropathol* 2008; **115**: 133–145.
12. Hasegawa M, Arai T, Akiyama H *et al.* TDP-43 is deposited in the Guam parkinsonism-dementia complex brains. *Brain* 2007; **130**: 1386–1394.
13. Uryu K, Nakashima-Yasuda H, Forman MS *et al.* Concomitant TAR-DNA-binding protein 43 pathology is present in Alzheimer disease and corticobasal degeneration but not in other tauopathies. *J Neuropathol Exp Neurol* 2008; **67**: 555–564.
14. Amador-Ortiz C, Lin WL, Ahmed Z *et al.* TDP-43 immunoreactivity in hippocampal sclerosis and Alzheimer's disease. *Ann Neurol* 2007; **61**: 435–445.
15. Josephs KA, Whitwell JL, Knopman DS *et al.* Abnormal TDP-43 immunoreactivity in AD modifies clinicopathologic and radiologic phenotype. *Neurology* 2008; **70**: 1850–1857.
16. Higashi S, Iseki E, Yamamoto R *et al.* Concurrence of TDP-43, tau and alpha-synuclein pathology in brains of Alzheimer's disease and dementia with Lewy bodies. *Brain Res* 2007; **1184**: 284–294.
17. Morris JC, Heyman A, Mohs RC *et al.* The Consortium to Establish a Registry for Alzheimer's Disease (CERAD). Part I. Clinical and neuropsychological assessment of Alzheimer's disease. *Neurology* 1989; **39**: 1159–1165.
18. Hyman BT, Trojanowski JQ. Editorial on consensus recommendations for the postmortem diagnosis of Alzheimer disease from the National Institute on Aging and the Reagan Institute Working Group on diagnostic criteria for the neuropathological assessment of Alzheimer disease. *J Neuropathol Exp Neurol* 1997; **56**: 1105–1118.
19. Sakurai A, Okamoto K, Yaguchi M *et al.* Pathology of the inferior olivary nucleus in patients with multiple system atrophy. *Acta Neuropathol* 2002; **103**: 550–554.
20. Mackenzie IR, Baborie A, Pickering-Brown S *et al.* Heterogeneity of ubiquitin pathology in frontotemporal lobar degeneration: classification and relation to clinical phenotype. *Acta Neuropathol* 2006; **112**: 539–549.
21. Cairns NJ, Bigio EH, Mackenzie IR *et al.* Neuropathologic diagnostic and nosologic criteria for frontotemporal lobar degeneration: consensus of the Consortium for Frontotemporal Lobar Degeneration. *Acta Neuropathol* 2007; **114**: 5–22.
22. Hu WT, Josephs KA, Knopman DS *et al.* Temporal lobar predominance of TDP-43 neuronal cytoplasmic

inclusions in Alzheimer disease. *Acta Neuropathol* 2008; **116**: 215–220.
23. Seibenhener ML, Babu JR, Geetha T, Wong HC, Krishna NR, Wooten MW. Sequestosome 1/p62 is a polyubiquitin chain binding protein involved in ubiquitin proteasome degradation. *Mol Cell Biol* 2004; **24**: 8055–8068.
24. Kuusisto E, Suuronen T, Salminen A. Ubiquitin-binding protein p62 expression is induced during apoptosis and proteasomal inhibition in neuronal cells. *Biochem Biophys Res Commun* 2001; **280**: 223–228.
25. Kuusisto E, Salminen A, Alafuzoff I. Early accumulation of p62 in neurofibrillary tangles in Alzheimer's disease: possible role in tangle formation. *Neuropathol Appl Neurobiol* 2002; **28**: 228–237.
26. Kuusisto E, Salminen A, Alafuzoff I. Ubiquitin-binding protein p62 is present in neuronal and glial inclusions in human tauopathies and synucleinopathies. *Neuroreport* 2001; **12**: 2085–2090.
27. Mizuno Y, Amari M, Takatama M, Aizawa H, Mihara B, Okamoto K. Immunoreactivities of p62, an ubiqutin-binding protein, in the spinal anterior horn cells of patients with amyotrophic lateral sclerosis. *J Neurol Sci* 2006; **249**: 13–18.
28. Pikkarainen M, Hartikainen P, Alafuzoff I. Neuropathologic features of frontotemporal lobar degeneration with ubiquitin-positive inclusions visualized with ubiquitin-binding protein p62 immunohistochemistry. *J Neuropathol Exp Neurol* 2008; **67**: 280–289.
29. Hiji M, Takahashi T, Fukuba H, Yamashita H, Kohriyama T, Matsumoto M. White matter lesions in the brain with frontotemporal lobar degeneration with motor neuron disease: TDP-43-immunopositive inclusions co-localize with p62, but not ubiquitin. *Acta Neuropathol* 2008; **116**: 183–191.

Neuroscience Letters 463 (2009) 87–92

Contents lists available at ScienceDirect

Neuroscience Letters

journal homepage: www.elsevier.com/locate/neulet

Phosphorylation-dependent TDP-43 antibody detects intraneuronal dot-like structures showing morphological characters of granulovacuolar degeneration

Ai Kadokura[a], Tsuneo Yamazaki[a,*], Satoko Kakuda[a], Kouki Makioka[a], Cynthia A. Lemere[b], Yukio Fujita[a], Masamitsu Takatama[c], Koichi Okamoto[a]

[a] Department of Neurology, Gunma University Graduate School of Medicine, 3-39-22 Showamachi, Maebashi, Gunma 371-8511, Japan
[b] Center for Neurologic Diseases, Brigham and Women's Hospital, Harvard Medical School, USA
[c] Geriatric Research Institute and Hospital, Gunma, Japan

ARTICLE INFO

Article history:
Received 13 March 2009
Received in revised form 1 June 2009
Accepted 11 June 2009

Keywords:
Alzheimer's disease
TDP-43
Phosphorylation
Granulovacuolar degeneration

ABSTRACT

TAR-DNA-binding protein 43 (TDP-43) was considered to be a disease-specific component of ubiquitin-positive and tau-negative inclusions in the brains of patients with frontotemporal lobar degeneration and amyotrophic lateral sclerosis (ALS). However, this protein also accumulates abnormally in neurons in other neurodegenerative diseases, including Alzheimer's disease (AD). Although the role of TDP-43 deposition in these diseases is not clear, abnormal phosphorylation of the protein is suggested to be a critical step in disease pathogenesis. In this study, we generated a new phosphorylation-dependent TDP-43 antibody and examined AD brain sections from temporal lobes, including the hippocampus and temporal neocortex, by immunohistochemistry. The antibody, called A2, specifically recognized phosphorylated TDP-43 in western blotting using ALS and AD specimens, detecting a strong 45 kDa band and several shorter fragments at around 25 kDa with smears. Immunohistochemistry demonstrated neuronal cytoplasmic inclusions in AD brain sections without staining nuclei that were normal physiological TDP-43 localization sites. These results were consistent with previous reports. However, intraneuronal dot-like structures were also intensely labeled by immunohistochemistry. These structures were observed in all the AD brain sections examined and also occurred in sections from the brains of aged subjects without AD pathologies. The morphological and immunohistochemical characteristics of these granular structures were compatible with those of granulovacuolar degeneration (GVD). The A2 antibody clearly and intensely detected granular structures distributed over the hippocampus, subiculum, parahippocampus and temporal neocortex. Thus, immunohistochemistry using phosphorylation-dependent TDP-43 antibodies would be a new useful tool for identifying GVD.

TAR-DNA-binding protein 43 (TDP-43) was first identified as a major component of ubiquitin-positive inclusions in brains from patients with sporadic frontotemporal lobar degeneration with ubiquitinated inclusions (FTLD-U), familial FTLD-U with progranulin gene mutations, and sporadic amyotrophic lateral sclerosis (ALS) [2,21]. Immunoblot analysis of the sarkosyl-insoluble, urea-soluble fraction extracted from the brains of patients affected with these disorders shows an abnormal TDP-43-immunoreactive band at 45 kDa. The electrophoretic mobility of this band changes after dephosphorylation, suggesting that abnormal phosphorylation occurs in accumulated TDP-43 [2,21]. Using specific antibodies to phosphorylate TDP-43, Hasegawa et al. found that the antibodies specifically stained the abnormal inclusions and did not stain nuclei that are the normal physiological TDP-43 localization sites detected by commercially available phosphorylation-independent antibodies [9]. They also found that abnormal phosphorylation of TDP-43 led to increases in its oligomerization and fibrillization *in vitro*. These results strongly indicate that abnormal phosphorylation of TDP-43 is a critical step in the pathogenesis of FTLD-U and ALS [9,13,22].

Abnormal TDP-43 immunoreactivity, however, has been detected in other neurodegenerative disorders, including Alzheimer's disease (AD) [1,10,11,14,15,28], Lewy body disease [23], corticobasal degeneration [28], Pick's disease [5], Guamanian parkinsonism-dementia complex [8], Guamanian ALS [7,8], hippocampal sclerosis [1], Huntington's disease [27], and argyrophilic grain disease [6]. We have previously examined TDP-43 inclusions in brains from patients with AD using a phosphorylation-independent antibody and found that TDP-43 has a region-specific distribution in the cortices and hippocampus [15]. To elucidate further the role of TDP-43 accumulation in AD, we

* Corresponding author. Tel.: +81 27 220 8064; fax: +81 27 220 8068.
E-mail addresses: tsuneoy@med.gunma-u.ac.jp, seiyai@showa.gunma-u.ac.jp (T. Yamazaki).

0304-3940/$ – see front matter © 2009 Published by Elsevier Ireland Ltd.
doi:10.1016/j.neulet.2009.06.024

generated a phosphorylation-specific anti-TDP-43 antibody and examined hippocampal sections from brains of patients with AD by immunohistochemistry. We found cytoplasmic phosphorylated TDP-43 inclusions; however, we also found unexpected intracellular granular immunoreactivity in hippocampal regions and in the temporal neocortices that showed morphologic characters consistent with granulovacuolar degeneration (GVD).

An antibody recognizing phosphorylated TDP-43 at positions 409 and 410 (A2) was made by injecting rabbits with the synthetic phosphopeptide, CSMDSKS(p)S(p)GWGM (amino acid residues 404–414 in human TDP-43), where S(p) represents phosphoserine. The peptide was conjugated at the amino terminus via a cysteine linkage to keyhole limpet hemocyanin (Pierce Biotechnology, Rockford, IL), using m-maleimidobenzoyl-*N*-hydroxysuccinimide ester as a coupling reagent. The rabbit antisera were purified by CNBr-activated Sepharose 4B (GE Healthcare, Buckinghamshire, UK) precoated with the synthetic nonphosphopeptide. The phosphorylation-independent TDP-43 antibody was purchased from Proteintech Group (10782-1-AP; Proteintech Group, Chicago, IL). Following antibodies were purchased; rabbit polyclonal anti-pS409/410 or pS403/404 (Cosmo Bio, Tokyo, Japan), guinea pig polyclonal anti-p62 (GP62N; Progen, Heidelberg, Germany), goat polyclonal anti-pSmad2/3 (sc-11769; Santa Cruz Biotechnology, Santa Cruz, CA), mouse monoclonal anti-SMI31 (Sternberger Monoclonals, Baltimore, MA), anti-ubiquitin (Chemicon, Temecula, CA) and anti-pGSK3 (5G-2F; Upstate Biotechnology, Lake Placid, NY).

The samples from the spinal cords of patients with ALS and controls, and from the hippocampal regions of patients with AD were extracted sequentially using low salt (LS; 10 mM Tris, pH 7.5, 5 mM EGTA, 1 mM DTT, 10% sucrose and a protease inhibitor cocktail), 1% Triton X-100 (TX; LS buffer + 1% Triton X-100 + 0.5 M NaCl), myelin (TX buffer containing 30% sucrose), 1% sarkosyl (LS buffer + 1% N-lauroyl-sarkosine + 0.5 M NaCl) and 7 M urea (7 M urea, 2 M thiourea, 4% CHAPS, 30 mM Tris, pH 8.5) buffers [26].

For dephosphorylation, the sarkosyl-insoluble, urea-soluble fractions were dialyzed against 30 mM Tris–HCl (pH 7.5) and incubated with lambda protein phosphatase (λPPase; New England Biolabs, Beverly, MA). For immunoblotting, protein samples were separated by 10% sodium dodecyl sulfate polyacrylamide gel electrophoresis and then electrotransferred onto a polyvinylidene difluoride membrane (Pall Corporation, East Hills, NY). After blocking with Blocking One P reagent (Nakarai Tesque, Kyoto, Japan) in Tris-buffered saline containing 0.1% Tween 20, membranes were incubated with A2 antibody overnight. After incubation with horseradish peroxidase-conjugated secondary antibody, labeling was detected by enhanced chemiluminescence (GE Healthcare, Buckinghamshire, UK).

Brain tissue was obtained from 16 subjects (average age: 74.8 years; 6 males, 10 females) who had died with clinically probable AD (CERAD C) [20] and AD-type pathologic changes that met the criteria for at least intermediate-probability AD [12]. Brain tissue from eight subjects who died at the age of 90 years or older and did not fulfill the pathological criteria of AD was also obtained.

Five-micrometer-thick sections of formalin-fixed, paraffin-embedded tissue from the medial temporal lobe including the hippocampus were immunostained with antibodies against phosphorylation-dependent TDP-43 (A2) using the streptavidin–biotin method (Histofine SAB-PO kit; Nichirei, Tokyo, Japan). In a subset of sections, immunostaining was also performed with rabbit polyclonal anti-phosphorylated TDP-43 antibodies recognizing pS409/410 or pS403/404 (Cosmo Bio). Immunoreactivity was visualized with 0.5 mg/ml 3,3′-diaminobenzidine tetrachloride (DAB) and 0.03% hydrogen peroxide (Dojin Laboratories, Kumamoto, Japan). All sections were counterstained with hematoxylin. For retrieving antigens in TDP-43 staining, the sections were autoclaved for 5 min. The specimens were observed under an Olympus BX60 microscope (Olympus, Tokyo, Japan) using DP Controller software.

For examining colocalization of phosphorylated TDP-43 with p62 that has been shown to be highly colocalized with TDP-43 inclusions in sections from the brains of patients with AD [15], sections were double labeled with the rabbit polyclonal anti-phosphorylation-dependent TDP-43 (A2) and guinea pig polyclonal anti-p62 (Progen) antibodies. Colocalization of phosphorylated TDP-43 with GVD markers was also examined in double-labeling studies with the rabbit polyclonal anti-phosphorylation-dependent TDP-43 (A2) and goat polyclonal anti-pSmad2/3 (Santa Cruz Biotechnology), mouse monoclonal anti-SMI31 (Sternberger Monoclonals), anti-ubiquitin (Chemicon) and anti-pGSK3 (Upstate Biotechnology) antibodies. After washing with phosphate-buffered saline, sections were treated with a cocktail of secondary antibodies: goat anti-rabbit Alexa Fluor 488 and goat anti-mouse Alexa Fluor 568, or goat anti-guinea pig Fluor 568 or donkey anti-rabbit Alexa Fluor 488 and donkey anti-goat Alexa Fluor 568 (Molecular Probes-Invitrogen, Eugene, OR). To avoid autofluorescence signaling, sections were pretreated with Sudan Black B for 5 min and rinsed in 70% ethanol. The specimens were examined under a microscope with confocal systems (FV1000; Olympus). The obtained images were further processed using Adobe Photoshop CS2 ver.9 (Adobe, San Jose, CA).

To investigate the specificity of our anti-phosphorylated TDP-43 antibody, 2A, immunoblots of sarkosyl-insoluble, urea-soluble fractions extracted from the spinal cords of subjects with sporadic ALS were conducted (Fig. 1A). As previously reported, a commercially available phosphorylation-independent TDP-43 antibody (Proteintech Group) revealed main bands of 43 kDa and weak bands of 45 kDa, corresponding to nonphosphorylated and phosphorylated TDP-43, respectively [2,9,13,22]. The phosphorylation-dependent antibody, A2, did not recognize the normal 43 kDa band; however, it revealed a single band at about 45 kDa and several additional smaller bands at around 25 kDa with smears in extracts from subjects with ALS (Fig. 1A). All the immunoreactive bands detected by A2 were abolished by dephosphorylation, which was performed with lambda protein phosphatase (Fig. 1B), suggesting that these bands were truly phosphorylated TDP-43 proteins. To examine immunoblots profiles of the A2 antibody in AD brains, medial temporal lobes of an AD brain were sequentially extracted as described in methods. Immunohistochemistry using the 2A antibody revealed that 17% of neurons contained cytoplasmic TDP-43 inclusions and 5% showed dot-like structures in the medial temporal lobes of this AD brain. As shown in Fig. 1C, although the phosphorylation-independent antibody detected the bands in several fractions, the 2A antibody recognized phosphorylated TDP-43 mainly in sarkosyl-insoluble, urea soluble fractions and no other intensely labeled bands were identified (Fig. 1C). As shown in Fig. 1D, the blotting patterns of AD samples were the same as those for ALS samples. Moreover, these 2A-positive bands were abolished by the dephosphorylation treatment (Fig. 1E).

Immunohistochemical staining with the 2A antibody showed distinct neuronal cytoplasmic labeling in the hippocampus and parahippocampus in some of the sections from brains of patients with AD, corresponding to neuronal cytoplasmic TDP-43 inclusions (Fig. 2A). The morphological characters of the inclusions were the same as those observed with phosphorylation-independent antibodies [15]. The phosphorylation-dependent antibody did not recognize normal nuclei, which are nonphosphorylated TDP-43 localization sites [9,13,22].

Interestingly, small dot-like structures in the neuronal cytoplasm were also intensely stained with the A2 antibody (Fig. 2A). These structures were observed mainly in pyramidal neurons in Sommer's sector of the hippocampus (Fig. 2B and C), with some

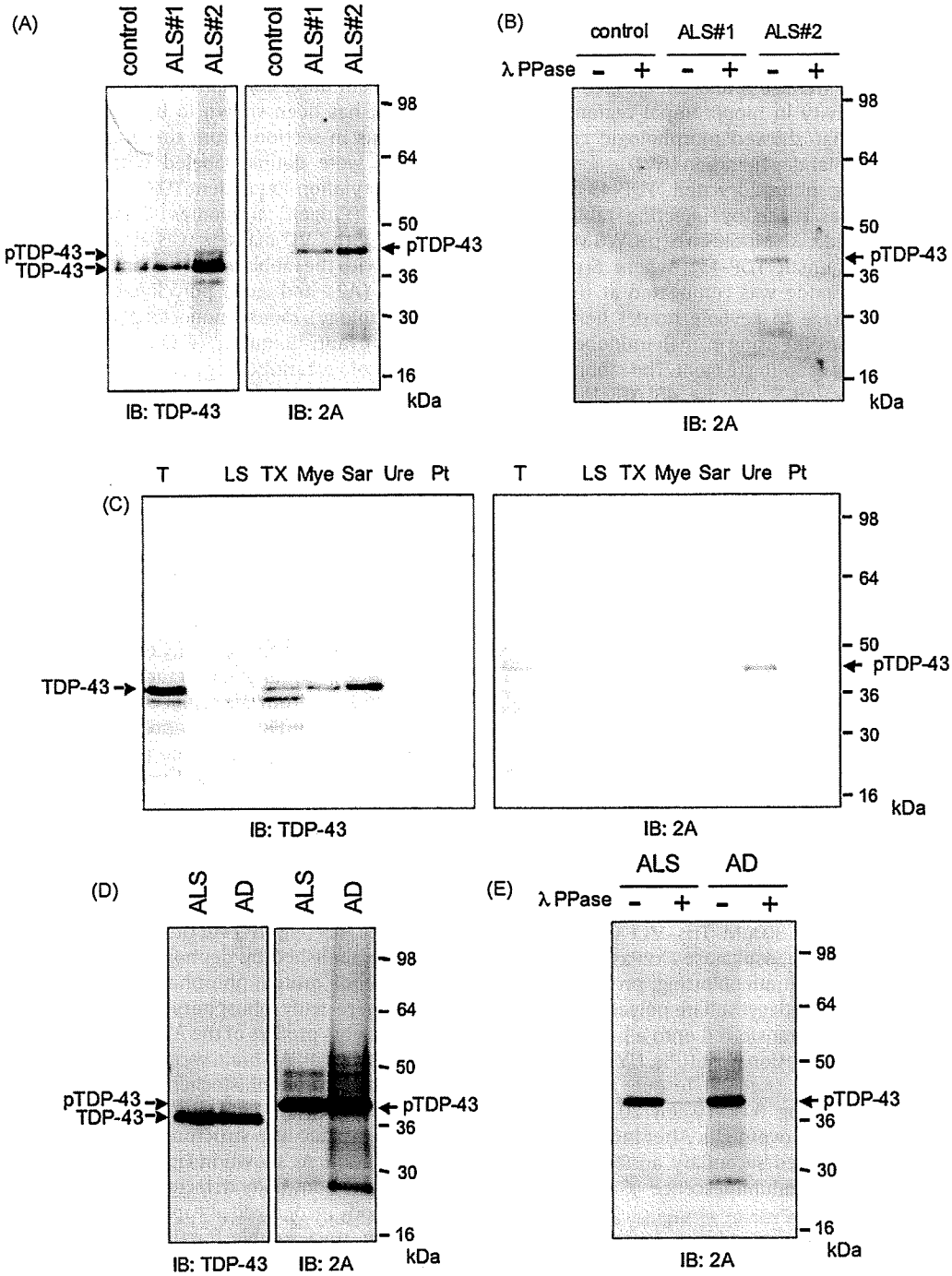

Fig. 1. Immunoblot analysis of sarkosyl-insoluble, urea-soluble fractions. (A; left panel) A commercially available phosphorylation-independent TDP-43 antibody (Proteintech Group) strongly detected bands at 43 kDa corresponding to nonphosphorylated TDP-43 in spinal cords from control and ALS samples. It also faintly identified phosphorylated TDP-43 bands at around 45 kDa only in ALS subjects. (A; right panel) In addition, the 2A antibody detected a single band at about 45 kDa and several smaller fragments at around 25 kDa with smears only in ALS samples. (B) The 45 kDa bands detected by the 2A antibody were abolished by dephosphorylation treatment. (C) Immunoblots of sequential extracts from an AD brain. Although nonphosphorylated TDP-43 was distributed in several fractions (C; left panel), the 2A antibody excessively reacted with full length phosphorylated TDP-43 mainly in the sarkosyl insoluble, urea soluble fraction of the AD brain (C; right panel). (D and E) The biochemical profiles of ALS brain samples were identical for AD hippocampal samples. IB, immunoblotting; pTDP-43, phosphorylated TDP-43; T, total homogenate; LS, low salt buffer soluble fraction; TX, 1% Triton-X buffer soluble fraction; Mye, myelin buffer soluble fraction; Sar, 1% sarkosyl-soluble fraction; Ure, sarkosyl-insoluble, urea-soluble fraction; Pt, urea-insoluble fraction.

in the subiculum (Fig. 2D) and parahippocampus (especially in entorhinal cortex) (Fig. 2E), and less in the temporal neocortex (Fig. 2F and G). These structures were not colocalized with neuronal TDP-43 cytoplasmic inclusions. In the hippocampus, these A2-immunoreactive dot-like structures were mainly observed around nuclei and located inside larger vacuoles (Fig. 2C). The granular structures detected in the parahippocampus and cortices were smaller in size and fewer in number than those observed in the hippocampus; however, A2-immunoreactive dot-like structures also occurred in surrounding vacuoles (Fig. 2E and G). The A2 immunoreactivity in these granular structures was observed in all sections that were examined from subjects with AD. An immunoabsorption study using the corresponding peptide completely abolished the immunoreactivity (data not shown). Our 2A antibody did not recognize other structures, such as neurofibrillary tangles in brain sections from subjects with AD. To examine

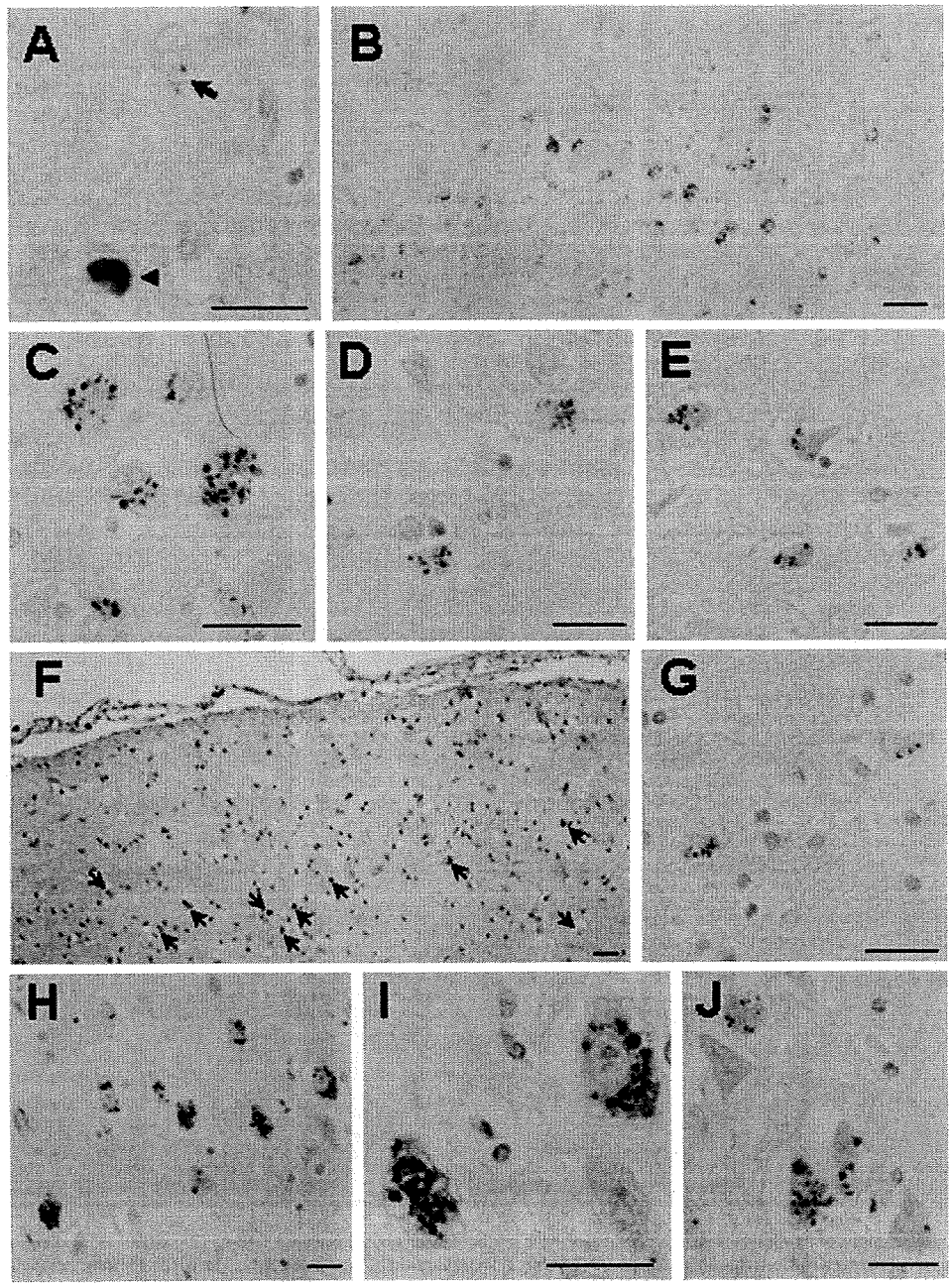

Fig. 2. (A) The phosphorylation-dependent TDP-43 A2 antibody detected intraneuronal inclusions in the parahippocampus of sections from the brain of an AD subject (arrowhead), and small dot-like structures in the cytoplasm were also labeled (arrow). Normal TDP-43 localization in nuclei was not stained by the A2 antibody. (B and C) Intracytoplasmic dot-like structures were distributed in the CA2 region of the hippocampus, (D) subiculum, (E) entorhinal cortex, and (F and G) occipitotemporal cortex. The same structures surrounded by vacuoles (C, D, E and G) were also detected by commercially available TDP-43 antibodies recognizing phosphorylation sites at positions 409/410 (H) and 403/404 (I) in the hippocampus. (J) The dot-like structures were also detected by the 2A antibody in the CA1 region of normal aged brains that did not fulfill AD criteria. Scale bars, 25 μm.

whether these granular staining was specific to our 2A antibody and the phosphorylation sites of TDP-43, we also used commercially available polyclonal antibodies that recognize the phosphorylation sites pS409/410 (Fig. 2H) and pS403/404 (Fig. 2I). These antibodies also stained neuronal dot-like structures (Fig. 2H and I).

The morphological characteristics of the 2A-positive cytoplasmic granular structures were similar to those for GVD [19]. To determine whether the immunopositive dot-like structures showed GVD characters, sections from the hippocampus of AD brains were double labeled with the 2A antibody and antibodies against p62 (Fig. 3A–C), the GVD marker protein, pSmad 2/3 (Fig. 3D–F) [3], SMI-31 (Fig. 3G–I) [25], ubiquitin (Fig. 3J–L) [24], or pGSK 3 (Fig. 3M–O) [18]. Colocalization rates, obtained by counting 50 2A-positive granules were 92.2% for p62, 100% for pSmad 2/3 and SMI-31, 60.3% for ubiquitin, and 50% for pGSK3. Thus, these reported GVD markers colocalized with 2A immunoreactivity, although their colocalization rates varied.

Because GVD occurs in AD brains and aged brains, brains from subjects who died at 90 years of age or older without displaying AD pathologies were also examined. As shown in Fig. 2J, the phosphorylation-dependent TDP-43 antibody also detected dot-like structures in the hippocampus of aged brains.

Abnormal phosphorylation of TDP-43 has been suggested to be a pathological event in FTLD-U and ALS [9,13,22]. In this study,

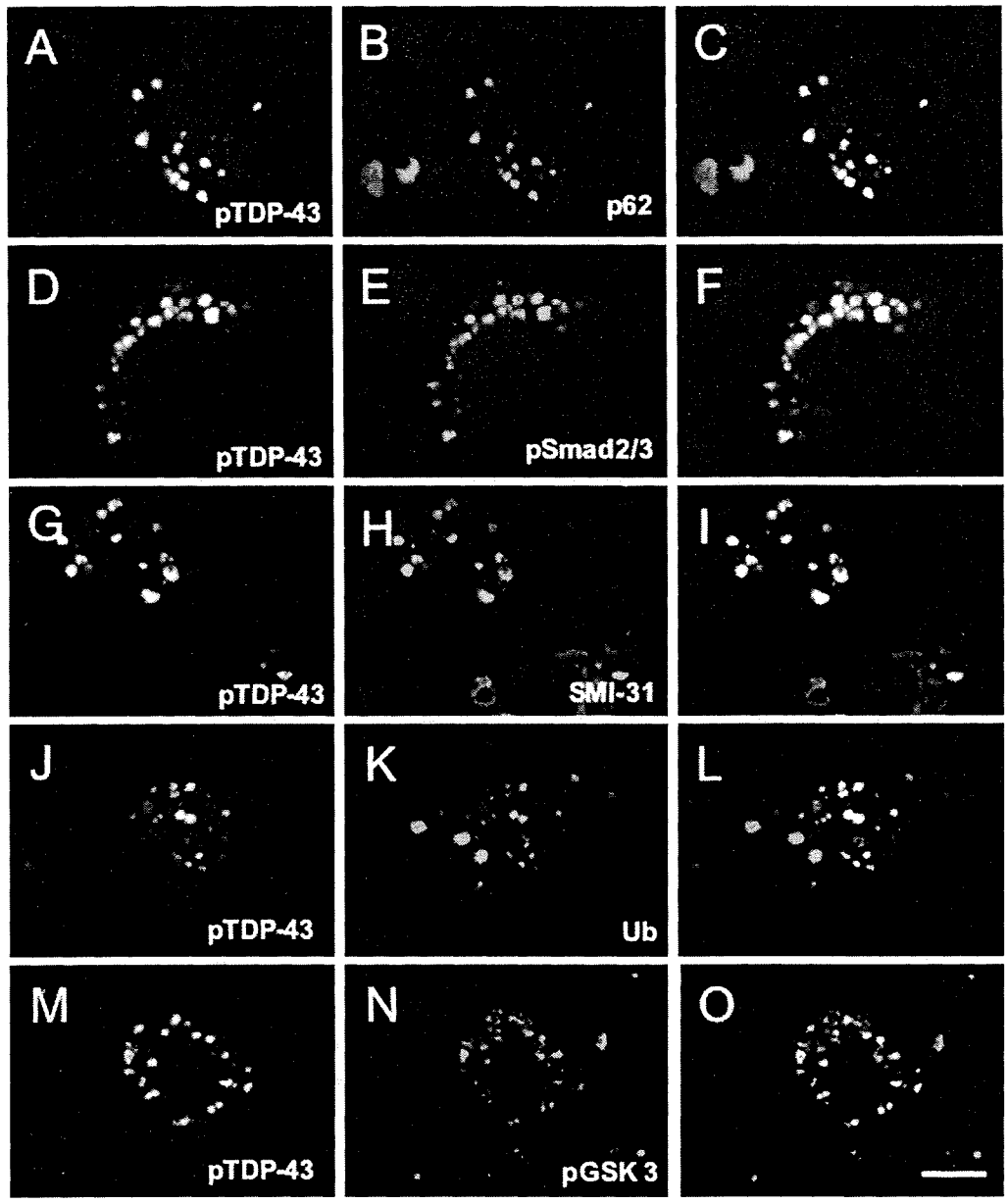

Fig. 3. Sections from the hippocampus of AD brains were double labeled with antibodies for phosphorylated TDP-43 (2A; pTDP-43) and antibodies for p62 (B) and various marker proteins of granulovacuolar degeneration including, pSmad 2/3 (E), SMI-31 (H), ubiquitin (K) and pGSK 3 (N). The pTDP-43 immunolabeling colocalized with immunolabeling for the various protein markers demonstrated by merged images (C, F, I, L and O), suggesting that the dot-like structures represent granulovacuolar degeneration. Scale bar, 10 μm.

we have produced a polyclonal antibody raised against a TDP-43 peptide phosphorylated at positions 409 and 410. In agreement with previous observations, the 2A antibody strongly recognized a 45 kDa full-length phosphorylated TDP-43 protein as well as shorter forms of the protein and smears on immunoblots [9,13,22]. These bands were abolished by dephosphorylation treatment. Thus, we concluded that the 2A antibody is specific for phosphorylated TDP-43, although it is not certain whether the appearance of these immunopositive bands is particular to ALS and AD samples [22]. In immunohistochemistry experiments with the 2A antibody and AD brain sections, abnormal TDP-43 inclusions in the neuronal cytoplasm were detected; however, nuclei, which are normal TDP-43 localization sites, were not labeled.

Interestingly, intraneuronal dot-like structures were also detected by the 2A antibody. To investigate the specificity of this staining, we carried out a series of experiments including an absorption study, immunoblotting using AD samples, and immunohistochemistry using additional polyclonal antibodies recognizing the same and other phosphorylation sites of TDP-43. Our findings indicated that the immunoreactivity in the dot-like structures was specific to phosphorylated TDP-43. Because previous studies, including our study using a commercially available phosphorylation-independent antibody (Proteintech Group and Abnova Corporation) that almost exclusively detects nonphosphorylated TDP-43 (Fig. 1A), have not reported the granular dot-like staining (data not shown), it is possible that these structures were composed of highly phosphorylated TDP-43 or truncated forms of the peptide lacking the epitopes recognized by the phosphorylation-independent antibodies.

The phosphorylated TDP-43-positive dot-like structures were also observed in sections of hippocampus from aged subjects without AD pathologies, and the morphological and immunohistochem-

ical characters of the granular structures were indistinguishable from those of GVD. Based on these ultrastructural observations, we previously reported that the small vacuoles of GVD were morphologically identical to autophagosomes [24]. Interestingly, recent *in vitro* studies have shown that functional multivesicular bodies, which are key compartments for efficient autophagic degradation, are required for TDP-43 clearance [4]. Additionally, overexpression of ubiquilin 1, which is a polyubiquitin–TDP-43 cochaperone, delivers TDP-43 to autophagosomes [16]. Moreover, in inclusion body myositis, which might be caused by alterations in autophagic degradation pathways, TDP-43 accumulation is found in rimmed vacuoles, which show autophagosomal characteristics [17,29]. These findings suggest that autophagosomes might be one of the intracellular compartments for TDP-43 degradation, and disruption of autophagic pathways might lead to TDP-43 accumulation in autophagosomes and its related compartments.

Phosphorylation-dependent TDP-43 antibodies specifically and intensely detected granular structures demonstrating GVD characters, even in the temporal neocortices. Although it has been reported that GVD is distributed outside of the hippocampal area [19], it is difficult to identify these structures by conventional methods. Thus, immunohistochemistry using the phosphorylation-dependent TDP-43 antibody would be a powerful new tool with which to identify GVD in brain tissue.

Acknowledgements

This study was supported by grants from the Ministry of Health, Labor and Welfare and the Ministry of Education, Culture, Sports, Science and Technology of Japan to K. Okamoto.

References

[1] C. Amador-Ortiz, W.L. Lin, Z. Ahmed, D. Personett, P. Davies, R. Duara, N.R. Graff-Radford, M.L. Hutton, D.W. Dickson, TDP-43 immunoreactivity in hippocampal sclerosis and Alzheimer's disease, Ann. Neurol. 61 (2007) 435–445.
[2] T. Arai, M. Hasegawa, H. Akiyama, K. Ikeda, T. Nonaka, H. Mori, D. Mann, K. Tsuchiya, M. Yoshida, Y. Hashizume, T. Oda, TDP-43 is a component of ubiquitin-positive tau-negative inclusions in frontotemporal lobar degeneration and amyotrophic lateral sclerosis, Biochem. Biophys. Res. Commun. 351 (2006) 602–611.
[3] K.A. Chalmers, S. Love, Neurofibrillary tangles may interfere with Smad 2/3 signaling in neurons, Neuropathol. Exp. Neurol. 66 (2007) 158–167.
[4] M. Filimonenko, S. Stuffers, C. Raiborg, A. Yamamoto, L. Malerød, E.M. Fisher, A. Isaacs, A. Brech, H. Stenmark, A. Simonsen, Functional multivesicular bodies are required for autophagic clearance of protein aggregates associated with neurodegenerative disease, J. Cell Biol. 179 (2007) 485–500.
[5] S.H. Freeman, T. Spires-Jones, B.T. Hyman, J.H. Growdon, M.P. Frosch, TAR-DNA binding protein 43 in Pick disease, J. Neuropathol. Exp. Neurol. 67 (2008) 62–77.
[6] H. Fujishiro, H. Uchikado, T. Arai, M. Hasegawa, H. Akiyama, O. Yokota, K. Tsuchiya, T. Togo, E. Iseki, Y. Hirayasu, Accumulation of phosphorylated TDP-43 in brains of patients with argyrophilic grain disease, Acta Neuropathol. 117 (2009) 151–158.
[7] F. Geser, M.J. Winton, L.K. Kwong, Y. Xu, S.X. Xie, L.M. Igaz, R.M. Garruto, D.P. Perl, D. Galasko, V.M. Lee, J.Q. Trojanowski, Pathological TDP-43 in parkinsonism-dementia complex and amyotrophic lateral sclerosis of Guam, Acta Neuropathol. 115 (2008) 133–145.
[8] M. Hasegawa, T. Arai, H. Akiyama, T. Nonaka, H. Mori, T. Hashimoto, M. Yamazaki, K. Oyanagi, TDP-43 is deposited in the Guam parkinsonism-dementia complex brains, Brain 130 (2007) 1386–1394.
[9] M. Hasegawa, T. Arai, T. Nonaka, F. Kametani, M. Yoshida, Y. Hashizume, T.G. Beach, E. Buratti, F. Baralle, M. Morita, I. Nakano, T. Oda, K. Tsuchiya, H. Akiyama, Phosphorylated TDP-43 in frontotemporal lobar degeneration and amyotrophic lateral sclerosis, Ann. Neurol. 64 (2008) 60–70.
[10] S. Higashi, E. Iseki, R. Yamamoto, M. Minegishi, H. Hino, K. Fujisawa, T. Togo, O. Katsuse, H. Uchikado, Y. Furukawa, K. Kosaka, H. Arai, Concurrence of TDP-43, tau and alpha-synuclein pathology in brains of Alzheimer's disease and dementia with Lewy bodies, Brain Res. 1184 (2007) 284–294.
[11] W.T. Hu, K.A. Josephs, D.S. Knopman, B.F. Boeve, D.W. Dickson, R.C. Petersen, J.E. Parisi, Temporal lobar predominance of TDP-43 neuronal cytoplasmic inclusions in Alzheimer disease, Acta Neuropathol. 116 (2008) 215–220.
[12] B.T. Hyman, J.Q. Trojanowski, Editorial on consensus recommendations for the postmortem diagnosis of Alzheimer's disease from the National Institute on Aging and the Reagan Institute Working Group on diagnostic criteria for the neuropathological assessment of Alzheimer disease, J. Neuropathol. Exp. Neurol. 56 (1997) 1105–1118.
[13] Y. Inukai, T. Nonaka, T. Arai, M. Yoshida, Y. Hashizume, T.G. Beach, E. Buratti, F.E. Baralle, H. Akiyama, S. Hisanaga, M. Hasegawa, Abnormal phosphorylation of Ser409/410 of TDP-43 in FTLD-U and ALS, FEBS Lett. 582 (2008) 2899–2904.
[14] K.A. Josephs, J.L. Whitwell, D.S. Knopman, W.T. Hu, D.A. Stroh, M. Baker, R. Rademakers, B.F. Boeve, J.E. Parisi, G.E. Smith, R.J. Ivnik, R.C. Petersen, C.R. Jack Jr., D.W. Dickson, Abnormal TDP-43 immunoreactivity in AD modifies clinicopathologic and radiologic phenotype, Neurology 70 (2008) 1850–1857.
[15] A. Kadokura, T. Yamazaki, C.A. Lemere, M. Takatama, K. Okamoto, Regional distribution of TDP-43 inclusions in Alzheimer disease (AD) brains: their relation to AD common pathology, Neuropathology, in press.
[16] S.H. Kim, Y. Shi, K.A. Hanson, L.M. Williams, R. Sakasai, M.J. Bowler, R.S. Tibbetts, Potentiation of ALS-associated TDP-43 aggregation by the proteasome-targeting factor, Ubiquilin 1, J. Biol. Chem. (2008), Epub ahead of print.
[17] B. Küsters, B.J. van Hoeve, H.J. Schelhaas, H. Ter Laak, B.G. van Engelen, M. Lammens, TDP-43 accumulation is common in myopathies with rimmed vacuoles, Acta Neuropathol. 117 (2009) 209–211.
[18] K. Leroy, A. Boutajangout, M. Authelet, J.R. Woodgett, B.H. Anderton, J.P. Brion, The active form of glycogen synthase kinase-3β is associated with granulovacuolar degeneration in neurons in Alzheimer's disease, Acta Neuropathol. 103 (2002) 91–99.
[19] S. Love, D.N. Louis, D.W. Ellison (Eds.), Granulovacuolar Degeneration. Greenfield's Neuropathology, Hodder Arnold, London, 2008, 1059 pp.
[20] J.C. Morris, A. Heyman, R.C. Mohs, J.P. Hughes, G. van Belle, G. Fillenbaum, E.D. Mellits, C. Clark, The Consortium to Establish a Registry for Alzheimer's Disease (CERAD). Part I. Clinical and neuropsychological assessment of Alzheimer's disease, Neurology 39 (1989) 1159–1165.
[21] M. Neumann, D.M. Sampathu, L.K. Kwong, A.C. Truax, M.C. Micsenyi, T.T. Chou, J. Bruce, T. Schuck, M. Grossman, C.M. Clark, L.F. McCluskey, B.L. Miller, E. Masliah, I.R. Mackenzie, H. Feldman, W. Feiden, H.A. Kretzschmar, J.Q. Trojanowski, V.M. Lee, Ubiquitinated TDP-43 in frontotemporal lobar degeneration and amyotrophic lateral sclerosis, Science 314 (2006) 130–133.
[22] M. Neumann, L.K. Kwong, E.B. Lee, E. Kremmer, A. Flatley, Y. Xu, M.S. Forman, D. Troost, H.A. Kretzschmar, J.Q. Trojanowski, V.M. Lee, Phosphorylation of S409/410 of TDP-43 is a consistent feature in all sporadic and familial forms of TDP-43 proteinopathies, Acta Neuropathol. 117 (2009) 137–149.
[23] H. Nakashima-Yasuda, K. Uryu, J. Robinson, S.X. Xie, H. Hurtig, J.E. Duda, S.E. Arnold, A. Siderowf, M. Grossman, J.B. Leverenz, R. Woltjer, O.L. Lopez, R. Hamilton, D.W. Tsuang, D. Galasko, E. Masliah, J. Kaye, C.M. Clark, T.J. Montine, V.M. Lee, J.Q. Trojanowski, Co-morbidity of TDP-43 proteinopathy in Lewy body related diseases, Acta Neuropathol. 114 (2007) 221–229.
[24] K. Okamoto, S. Hirai, T. Iizuka, T. Yanagisawa, M. Watanabe, Reexamination of granulovacuolar degeneration, Acta Neuropathol. 82 (1991) 340–345.
[25] A. Probst, M.C. Herzig, C. Mistl, S. Ipsen, M. Tolnay, Perisomatic granules (non-plaque dystrophic dendrites) of hippocampal CA1 neurons in Alzheimer's disease and Pick's disease: a lesion distinct from granulovacuolar degeneration, Acta Neuropathol. 102 (2001) 636–644.
[26] D.M. Sampathu, M. Neumann, L.K. Kwong, T.T. Chou, M. Micsenyi, A. Truax, J. Bruce, M. Grossman, J.Q. Trojanowski, V.M. Lee, Pathological heterogeneity of frontotemporal lobar degeneration with ubiquitin-positive inclusions delineated by ubiquitin immunohistochemistry and novel monoclonal antibodies, Am. J. Pathol. 169 (2006) 1343–1352.
[27] C. Schwab, T. Arai, M. Hasegawa, S. Yu, P.L. McGeer, Colocalization of transactivation-responsive DNA-binding protein 43 and huntingtin in inclusions of Huntington disease, J. Neuropathol. Exp. Neurol. 67 (2008) 1159–1165.
[28] K. Uryu, H. Nakashima-Yasuda, M.S. Forman, L.K. Kwong, C.M. Clark, M. Grossman, B.L. Miller, H.A. Kretzschmar, V.M. Lee, J.Q. Trojanowski, M. Neumann, Concomitant TAR-DNA-binding protein 43 pathology is present in Alzheimer's disease and corticobasal degeneration but not in other tauopathies, J. Neuropathol. Exp. Neurol. 67 (2008) 555–564.
[29] C.C. Weihl, P. Temiz, S.E. Miller, G. Watts, C. Smith, M. Forman, P.I. Hanson, V. Kimonis, A. Pestronk, TDP-43 accumulation in inclusion body myopathy muscle suggests a common pathogenic mechanism with frontotemporal dementia, J. Neurol. Neurosurg. Psychiatry 79 (2008) 1186–1189.

Variations in the effects on synthesis of amyloid β protein in modulated autophagic conditions

Kouki Makioka, Tsuneo Yamazaki, Satoko Kakuda and Koichi Okamoto

Department of Neurology, Gunma University Graduate School of Medicine, Maebashi, Gunma, Japan

Objective: *Autophagy, the intracellular breakdown system for proteins and some organelles, is considered to be important in neurodegenerative disease. Recent reports suggest that autophagy plays an important role in Alzheimer's disease pathogenesis and autophagic vacuoles (AVs) may be sites of amyloid β protein (Aβ) generation. We attempted to determine if imposed changes in autophagic activity are linked to Aβ generation and secretion in cultured cells.*

Methods: *We used Chinese hamster ovary cells, stably expressing wild-type APP 751. We treated the cells with three known autophagy modulating conditions, rapamycin treatment, U18666A treatment and cholesterol depletion.*

Results: *All the three conditions resulted in increased levels of LC3-II by western blotting, together with an increase in the number of LC3-positive granules. However, the effects on Aβ production were inconsistent. The rapamycin treatment increased Aβ production and secretion, but the other two conditions had opposite effects. When the level of phosphorylation of the mammalian target of rapamycin (mTOR) was measured, down-regulation of phosphorylated mTOR levels was observed only in rapamycin-treated cells. The LC3-positive granules in the U18666A-treated and cholesterol-depleted cells were different from those in rapamycin-treated cells in terms of number, size and distribution, suggesting that degradative process from autophagosomes to lysosomes was disturbed.*

Discussion: *The biochemical pathways leading to autophagy and the generation of AVs appear to be different in cells treated by the three methods. These differences may explain why the similar autophagic status determined by LC3 immunoreactivities does not correlate with Aβ generation and secretion.* [Neurol Res 2009; **31**: 959–968]

Keywords: Autophagy; Alzheimer's disease; amyloid β protein (Aβ); cholesterol; Niemann–Pick disease type C

INTRODUCTION

Alzheimer's disease (AD) is an age-related neurodegenerative disorder characterized by progressive dementia. The morphological hallmarks are senile plaques, extracellular deposits of amyloid β-protein (Aβ) fibrils and neurofibrillary tangles (NFTs) containing hyperphosphorylated tau[1,2]. Aβ deposition in brains is considered to have a pivotal role in AD pathogenesis. Aβ is cleaved from the β-amyloid precursor protein (APP) by two consecutively working enzymes, β secretase and γ secretase[1,2]. Aβ has two major subspecies, Aβ40 ending in Val at position 40 of the Aβ amino acid sequence and Aβ42 ending in Ala at position 42. Aβ42 is more likely to aggregate than Aβ40[1,2]. Several cellular Aβ production sites have been proposed, including the endoplasmic reticulum–Golgi apparatus, plasma membrane, endosomes, lipid rafts and lysosomes[3], but the precise sites where Aβ is produced are unknown.

Autophagy may have an important role in AD pathogenesis, and autophagosomes could be one of the Aβ generation sites[4–6]. Autophagy is a constitutive mechanism for the turnover of cytoplasmic components. It is activated under certain conditions, including nutritional deprivation[7], which results in part of the cytoplasm being degraded by lysosomes. Microtubule-associated protein, light-chain 3 (LC3), a mammalian homologue of yeast Atg8, has been used as a specific marker to monitor autophagy. Upon induction of autophagy, a cytosolic form of LC3 (LC3-I) is conjugated to phosphatidylethanolamine to form the LC3–phosphatidylethanolamine conjugate (LC3-II) that is inserted into the autophagosomal membrane. Autophagosomes fuse with lysosomes to form autolysosomes and lysosomal hydrolases break down the intra-autophagosomal components. At the same time, the LC3-II in the autolysosomal lumen is degraded. Because the lysosomal turnover of the autophagosomal marker LC3-II thus reflects autophagic activity, the detection of LC3 by immunoblotting or immunofluorescence is a reliable method for monitoring autophagy and autophagy-related processes[8].

Correspondence and reprint requests to: T. Yamazaki, Department of Neurology, Gunma University Graduate School of Medicine, 3-39-22 Showa-machi, Maebashi, Gunma 371-8511, Japan. [tsuneoy@med.gunma-u.ac.jp] Accepted for publication November 2008.

10.1179/174313209X395463

Nixon *et al.* used electron microscopy to show that autophagic vacuoles (AVs), including double-membrane-limited autophagosomes and single membrane autophagolysosomes, accumulated in dystrophic neurites in AD and presenilin 1 (PS1)/APP mouse models of β-amyloidosis brains[9,10]. Purified AVs contained APP and β-cleaved APP and were highly enriched in the γ-secretase complex[5]. Inducing or inhibiting autophagy in neuronal and non-neuronal cells by modulating the mammalian target of rapamycin (mTOR) kinase elicited parallel changes in AV proliferation and Aβ production. These authors concluded from these results that autophagy is activated and that it is abnormal in AD. In contrast, Pickford *et al.*[6] report a reduction in the levels of beclin-1 in AD brains, an important component in autophagy. They also demonstrated that beclin-1 deficiency in APP transgenic mice reduced autophagy, accelerated extracellular deposition and intracellular accumulation of Aβ and resulted in neurodegeneration. Beclin-1 overexpression in APP transgenic mice reduced extracellular deposition and intracellular accumulation of Aβ. They concluded that beclin-1 deficiency disrupts neuronal autophagy in AD by modulating Aβ generation and accumulation.

Although these studies indicate that autophagy may be important in AD pathogenesis, whether autophagy is induced or disrupted in the disease process is unknown. One important issue to be clarified is whether the induction of autophagy inevitably elicits parallel changes in AV proliferation and Aβ production. To examine this issue, we compared both intracellular and secreted Aβ levels under several known conditions known to induce autophagy, including cholesterol depletion and disruption of cholesterol transport in cultured cells.

MATERIALS AND METHODS

Cell culture and treatment

Chinese hamster ovary cells, stably expressing wild-type APP 751 (7WD10) were grown and maintained in Dulbecco's modified Eagle's medium (DMEM) containing 100 U/ml penicillin G sodium, 100 μg/ml streptomycin sulfate, 0.2 mg/ml G418 sulfate and 10% fetal bovine serum[9]. These cells were generous gifts from Dr E. H. Koo (Department of Neuroscience, University of California, San Diego).

The rapamycin treatment consisted of adding 0.2 μg/ml rapamycin (Sigma-Aldrich, St Louis, MO, USA) to the media and cultured for 27 hours[10]. The U18666A treatment consisted of culturing the cells in media containing 3 μg/ml U18666A (Biomol, Plymouth Meeting, PA, USA) for 24 hours[11]. For the cholesterol depletion study, a monolayer of 7WD10 cells was washed twice with phosphate-buffered saline (PBS) and cultured in DMEM with 10% lipoprotein-deficient fetal calf serum (LPDS) in the presence of 20 μM mevastatin and 230 μM mevalonate (Sigma-Aldrich) for 48 hours[11]. The cellular free cholesterol content was determined using a Determinor L FC kit (Kyowa Medix, Tokyo, Japan). For amino acid starvation, the cells were incubated in Hanks' balanced salt solution for 6 hours. For inhibiting the autophagy induced by amino acid starvation, the cells were cultured in the media containing 100 nM wortmannin (Sigma-Aldrich), a selective inhibitor of classical PI3-kinase (PI3K), for 6 hours[12,13].

Antibodies

Monoclonal antibodies against Aβ, 6E10 (Signet Laboratories, Dedham, MA, USA) and 82E1 (IBL, Takasaki, Japan) were purchased and used for immunoprecipitation and western blotting, respectively. Polyclonal LC3 antibody was prepared by immunization of rabbits using a synthetic peptide corresponding to the N-terminal 14 amino acids of LC3 (PSDRPFKQRRSFAD) plus an additional cysteine[14,15]. Another anti-LC3 polyclonal antibody was kindly provided by Dr Y. Uchiyama (Department of Cell Biology and Neurosciences, Osaka University Graduate School of Medicine) and used for the immunocytochemical studies[16]. Anti-β-actin (Abcam, Cambridge, UK), anti-C-terminal of APP (Calbiochem, Darmstadt, Germany), anti-phospho-mTOR (Ser. 2448) (Cell Signaling, Danvers, MA, USA) and anti-beclin-1 (Santa Cruz Biotechnology, Santa Cruz, CA) antibodies were obtained commercially.

Immunoprecipitation and western blotting

To detect secreted Aβ, the conditioned media were treated with 6E10 in the presence of complete protease inhibitors (Roche Diagnostics GmbH, Mannheim, Germany) for 3 hours at 4°C, followed by incubation with protein G-Sepharose 4 Fast Flow (GE Healthcare Bio-sciences AB, Uppsala, Sweden) for 1.5 hours at 4°C. The immunoprecipitated protein was extracted in the Ramuri sample buffer and subjected to western blotting[17]. To detect intracellular Aβ, the cells were harvested either by scraping or 0.25% trypsin treatment and homogenized with Tris-buffered saline (TS; pH 7.4) containing complete protease inhibitors. The homogenates were delipidated by chloroform/methanol treatments, then extracted with 70% formic acid[11]. The resulting samples were subjected to western blotting using anti-Aβ antibody. Preliminary studies showed no difference in the levels of Aβ in specimens harvested either by scraping or trypsin treatment. Samples were separated on 12.5% Tris/Tricine gels and transferred to a nitrocellulose membrane, followed by boiling in PBS for 5 minutes to enhance the sensitivity for detecting Aβ[18]. The homogenates were separated on 15% or 10% SDS-polyacrylamide gels and transferred to polyvinylidene difluoride membranes for the detection of LC3, APP, beclin-1 and phospho-mTOR. The bound antibodies were observed using enhanced chemiluminescence (Amersham Bioscience, Piscataway, NJ, USA). The bands were visualized using LAS-3000 (Fujifilm, Tokyo, Japan) and the intensity of the bands was quantified using Multi Gauge Ver 3.0 (Fujifilm). Aβ, phosphorylated mTOR and beclin-1 levels in treated cells were expressed as a ratio relative to those in

corresponding nontreated controls at each time, and the data were statistically analysed using a *t*-test.

To quantify the changes in the Aβ42/Aβ40 ratio in secreted Aβ, we used the Human β Amyloid (1–40) ELISA Kit Wako II (BAN50/BA27(F(ab')2)) and the Human β Amyloid (1–42) ELISA Kit Wako (BAN50/BC05(Fab')) (Wako Pure Chemical Industries, Osaka, Japan).

Immunocytochemistry

Cells on coverslips were fixed in 4% neutral phosphate-buffered formaldehyde for 20 minutes at room temperature, rinsed in PBS and permeabilized with 0.1% Triton X-100 in PBS for 5 minutes. After blocking with 10% fetal bovine serum in PBS for 30 minutes, the cells were incubated with anti-LC3 antibody overnight at 4°C, followed by rinsing in PBS and 2 hours incubation with anti-rabbit IgG secondary antibody conjugated to Alexa Fluor 488 (Invitrogen, Carlsbad, CA, USA). The coverslips were mounted using a drop of Vectashield (Vector Laboratories, Burlingame, CA, USA) and examined under an Olympus BX50 microscope using DP Controller (Olympus, Tokyo, Japan). Images were prepared for presentation using Adobe Photoshop 6.0.

RESULTS

Rapamycin treatment increased AVs, with increases in both secreted and intracellular Aβ levels

We first reexamined the reported effects of rapamycin on the number of AVs and Aβ production[5]. After incubation with rapamycin, the LC3-II level was apparently increased compared with that in untreated controls (*Figure 1A*). Immunocytochemical staining using anti-LC3 antibody also revealed the appearance of granular structures in treated cells, suggesting that the treatment had induced the AVs (*Figure 1E,F*). Careful observation showed that most of the LC3-positive granules were located around the nuclei and were relatively rare (*Figure 1F*). Although the β-actin and APP expression levels were unchanged with this treatment (*Figure 1B*), the secreted Aβ level was apparently increased (2.71 ± 0.95, $p<0.01$, $n=6$) (*Figure 1C*). The levels of Aβ42 and Aβ40 were quantified using sensitive ELISA[5]. The ratio of Aβ42 to total Aβ was 9.75 ± 0.54% in control and 10.2 ± 0.99% in treated cells. Thus, the rapamycin treatment did not appear to affect the population of Aβ subspecies.

We tested the possibility that rapamycin treatment may fail to cause Aβ overproduction, but alter Aβ trafficking routes resulting in enhanced secretion, by examining changes in intracellular Aβ level after treatment. Results showed that the total intracellular Aβ level extracted with 70% formic acid was also increased by the treatment (1.79 ± 0.30, $p<0.01$, $n=6$) (*Figure 1D*). To exclude the possibility that secreted Aβ attached to the plasma membrane, resulting in the detection of high levels of Aβ in cell homogenates, the cells were harvested using 0.25% trypsin instead of scraping cells with a rubber scraper. However, the results were identical (data not shown). Finally, we quantified the blotting data by densitometoric measurements, and the statistically significant increases in both secreted and intracellular Aβ levels because of autophagic induction were validated (*Figure 1C,D*).

U18666A treatment increased AVs and decreased both secreted and intracellular Aβ levels

Increased autophagy may be involved in the pathogenesis of the Niemann–Pick disease type C (NPC)[19,20]. NPC is an autosomal recessive neurovisceral storage disease[21] characterized by the presence of numerous foamy cells in the bone marrow and visceral organs including the brain. Its hallmark is an intracellular accumulation of unesterified cholesterol and other lipids, especially sphingolipids, in vacuoles resembling late endosomes[22]. NPC has been of interest to AD investigators because it is one of the very few disorders in which NFTs robustly form in the brain without tau mutations or Aβ deposition[23]. NPC phenotypes are known to be generated in cultured cells by type 2 amphipheles such as U18666A, and this methodology has been widely used to model NPC cells[24]. These observations prompted us to examine if increased AVs in NPC cells is associated with augmented Aβ secretion and production.

As previously reported[25], the LC3-II level was increased by with U18666A treatment (*Figure 2A*). The appearance of LC3-positive granules was also confirmed by immunocytochemistry (*Figure 2E,F*). However, in regard to the number of LC3-positive granules, more immunoreactive structures were observed per cell compared with those in rapamycin-treated cultures (*Figures 1F* and *2F*). Moreover, the sizes of LC3-positive structures varied and were distributed throughout the cytoplasm, not only around the nuclei (*Figure 2F*). The β-actin and APP expression levels were unchanged by the treatment (*Figure 2B*). However, in contrast to rapamycin treatment, both secreted and intracellular Aβ levels were significantly decreased in NPC model cells (0.62 ± 0.24, $p<0.02$, $n=6$; 0.46 ± 0.17, $p<0.01$, $n=6$) (*Figure 2C,D*). As previously described, the viability of treated cells was not altered by this treatment[26]. The observed decrease in Aβ levels could not therefore be attributed to the vulnerability of the treated cells.

Cellular cholesterol depletion increased AVs and in this condition both secreted and intracellular Aβ levels were decreased

Cheng *et al.*[25] showed that cellular cholesterol depletion induces an increase in AVs in cultured cells. We therefore investigated this effect on Aβ secretion and production. A monolayer of 7WD10 cells was cultured in DMEM with 10% LPDS in the presence of mevastatin and mevalonate for 48 hours[11]. This cholesterol starvation protocol resulted in a 27.9 ± 12.7% decrease in the total cellular cholesterol level. In these treated cells, the LC3-II level clearly increased, as previously reported (*Figure 3A*), and the emergence of LC3-positive granules was confirmed by immunocytochemistry (*Figure 3E,F*). Again, the number of LC3-positive granules was larger than that seen in rapamycin-treated cells, and the sizes

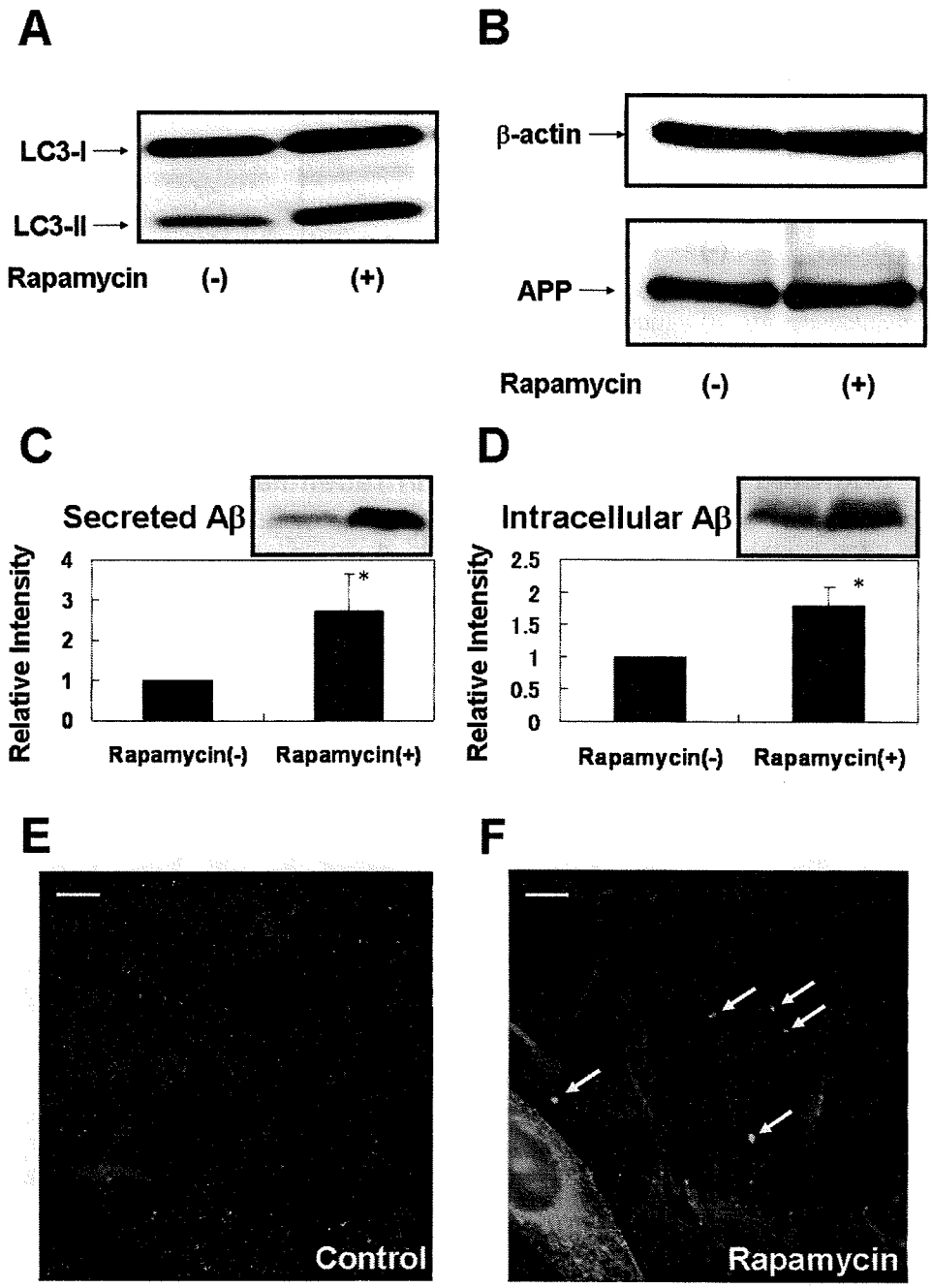

Figure 1: (**A**) LC3-II levels increased after incubation with rapamycin for 27 hours, compared with the untreated control. Immunocytochemical study using anti-LC3 antibody also showed granular structures in treated cells, suggesting that AVs appear due to the treatment. (**B**) Although the level of β-actin and APP expression was unchanged with this treatment, both (**C**) secreted and (**D**) intracellular Aβ levels increased (*$p<0.01$). These results are expressed as a ratio relative to those in untreated controls at each point. Data shows mean ± SD for six independent experiments. Immunocytochemical staining: (**E**) control and (**F**) rapamycin (bars=10 μm)

and locations were more varied (*Figure 3F*). Under this experimental condition, the β-actin, the APP levels (*Figure 3B*) and cell viability were not significantly altered, as previously reported[11]. However, described above, the secreted and intracellular Aβ levels were significantly decreased in cells showing increased AVs (0.63 ± 0.25, $p<0.02$, $n=6$. 0.52 ± 0.08, $p<0.01$, $n=6$) (*Figure 3C,D*).

Up-regulated Aβ levels may depend on the phosphorylation states of mTOR

The precise mechanism of autophagy induction in mammalian cells is not understood. However, the dephosphorylation of mTOR and increased expression of beclin-1 are considered to be independently involved in this process[27]. To discover why, we obtained contradictory results on Aβ secretion and intracellular

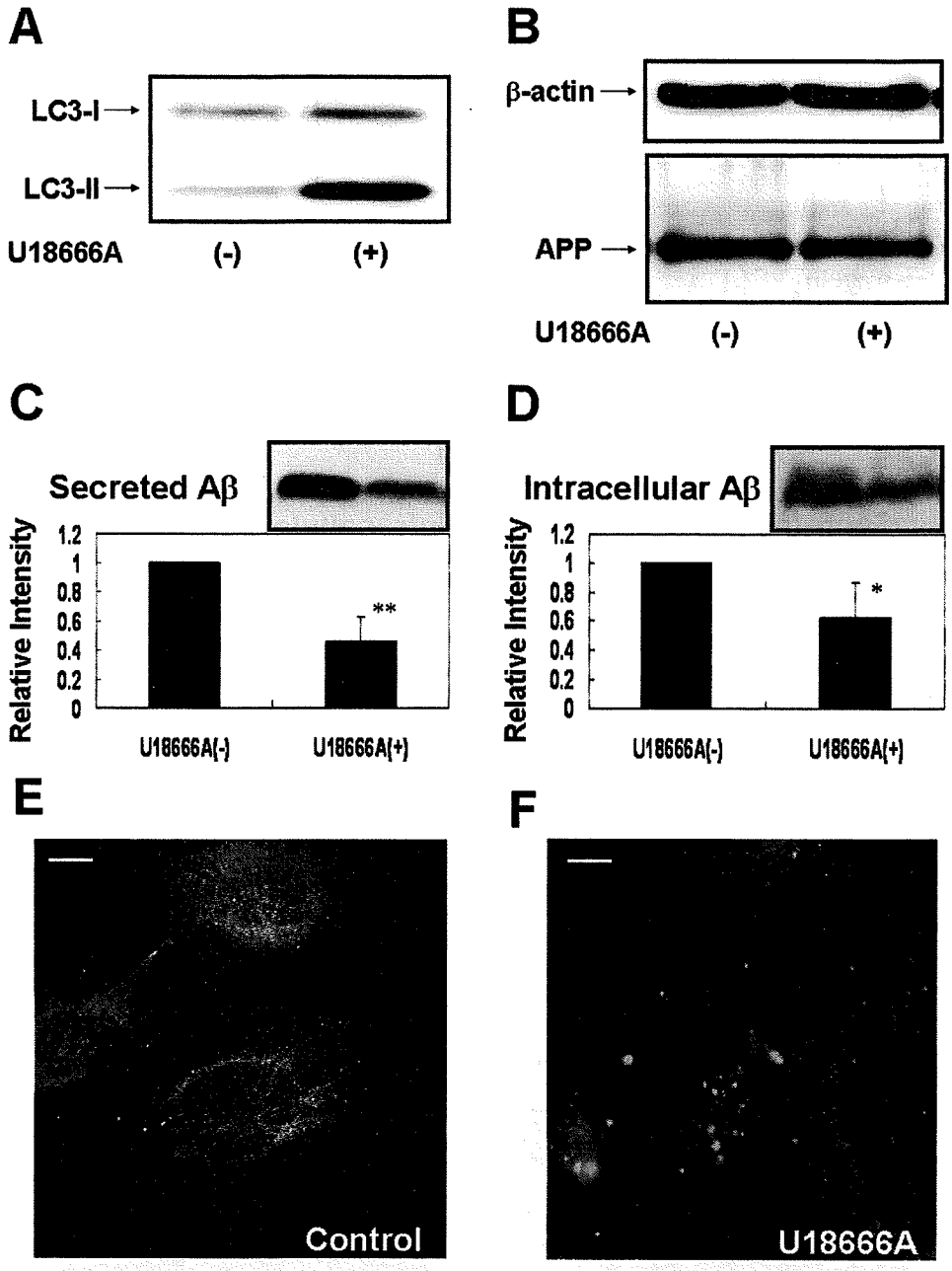

Figure 2: (**A**) After incubation with U18666A for 24 hours, LC3-II levels increased, together with the appearance of LC3-positive granules. This result was confirmed by immunocytochemistry. More immunoreactive structures were present per cell than in rapamycin-treated cells (*Figures 1F* and *2F*). The sizes of the LC3-positive structures were varied and distributed throughout the cytoplasm (*Figure 2F*). (**B**) The β-actin and APP level was not altered by the treatment. Both (**C**) secreted and (**D**) intracellular Aβ levels were significantly decreased in the treated cells (*$p<0.01$, **$p<0.02$). These results are expressed as a ratio relative to those from corresponding untreated controls at each time point. Data points are the means ± SD from six independent experiments. Immunocytochemical staining: (**E**) control and (**F**) U18666A (bars=10 μm)

Aβ using different AVs increasing methods, the levels of phosphorylated mTOR and beclin-1 were examined. As shown in *Figure 4A*, the level of phosphorylated mTOR decreased in the rapamycin-treated cells but remained unchanged in the U18666A-treated and cholesterol-depleted cells. Beclin-1 levels were not statistically altered by any of the treatments, although the beclin-1 level tended to slightly increase in the U18666A-treated cells ($p=0.3$, $n=4$) (*Figure 4B*).

To confirm the role of phosphorylated mTOR on Aβ levels, the cells were treated with wortmannin, a selective inhibitor of classical PI3K[12,13], resulting in the inhibition of mTOR dephosphorylation[28] and the suppression of autophagy induced by amino acid

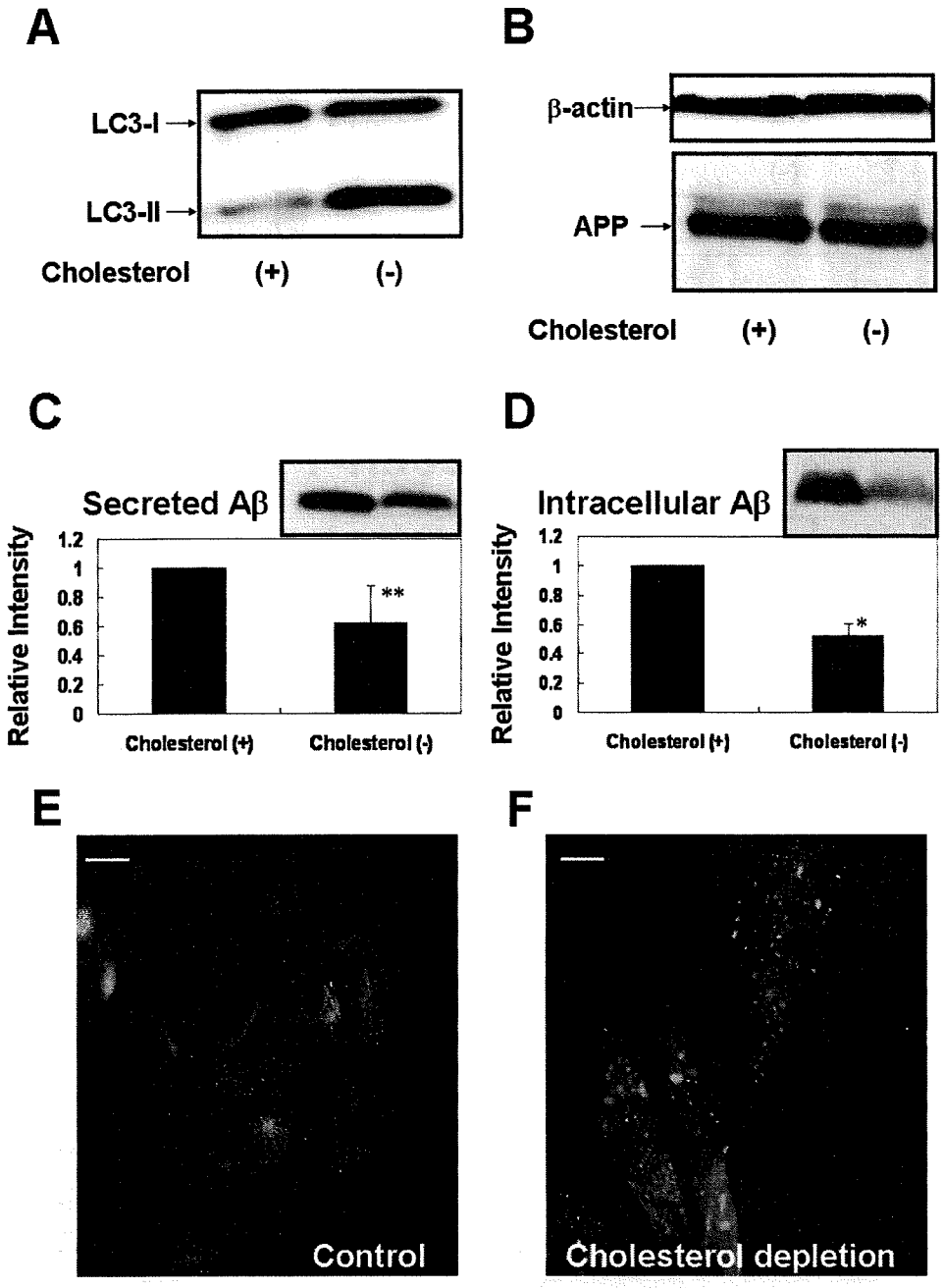

Figure 3: (**A**) After incubation in DMEM with 10% LPDS in the presence of 20 μM mevastatin and 230 μM mevalonate for 48 hours, LC3-II levels increased and immunocytochemistry showed the appearance of LC3-positive granules. The number of LC3-positive granules was higher than in rapamycin-treated cells, and they varied in both size and locations (*Figures 1F* and *3F*). (**B**) The β-actin and APP level remained unchanged by the treatment, but both (**C**) secreted and (**D**) intracellular Aβ levels were significantly lower as shown in U18666A-treated cells (*$p<0.01$, **$p<0.02$). The results are expressed as a ratio relative to those from corresponding untreated controls at each time point. Data shows mean ± SD from six independent experiments. Immunocytochemical staining: (**E**) control and (**F**) cholesterol depletion (bars=10 μm)

starvation[29]. Wortmannin (100 nM) evidently suppressed the LC3-II levels in starved cells (*Figure 4C*). The increased level of LC3-II was not suppressed in the U18666A-treated cells (*Figure 4D*), and the decreased levels of Aβ secretion and production were unchanged with this treatment (*Figure 4E*).

DISCUSSION

Because the level of LC3-II correlates with the number of autophagosomes, immunoblotting for LC3 can be used to measure autophagic activity[14]. Direct determination of LC3 localization within granular structures is also a widely adopted method for measuring autophagic

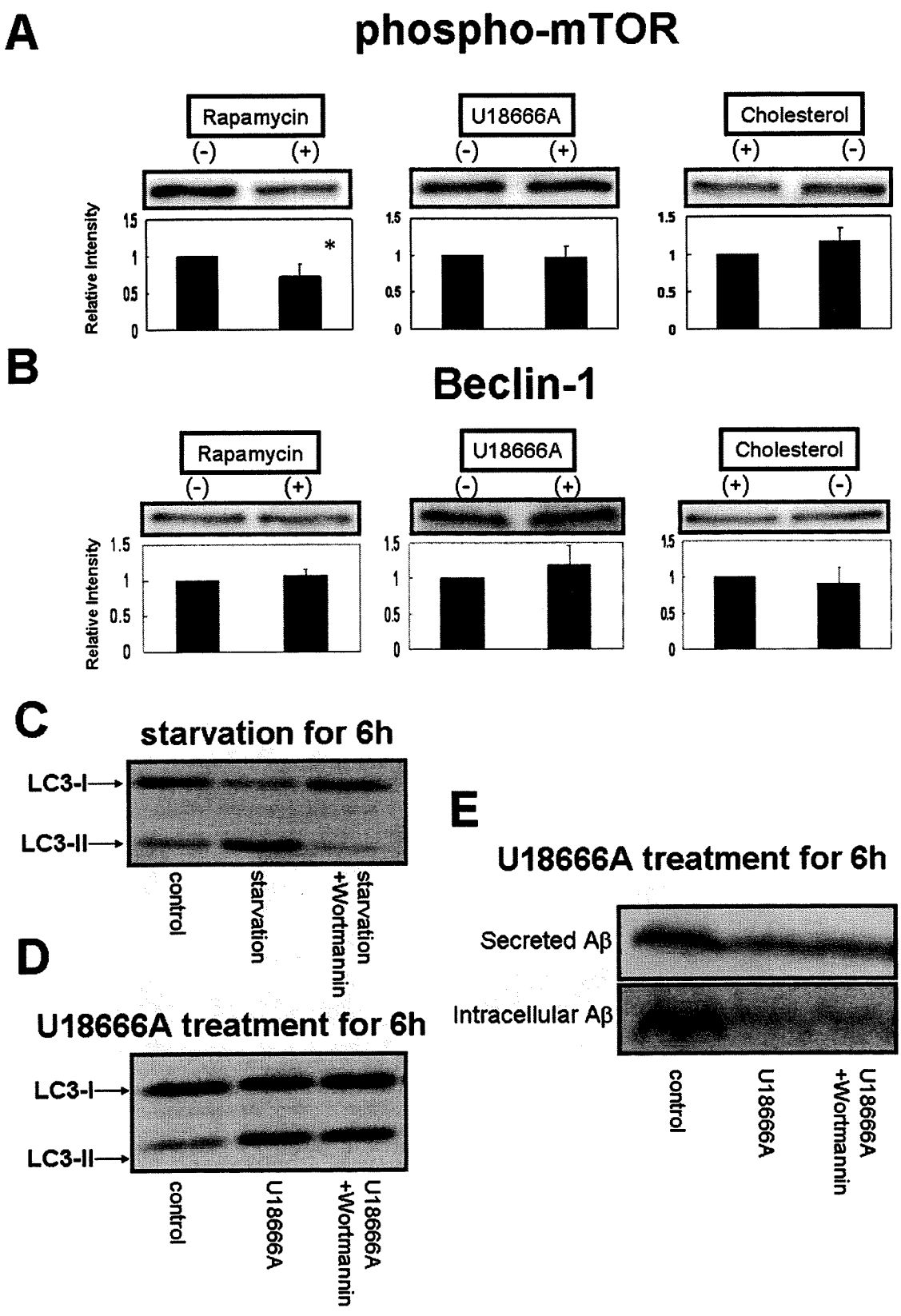

Figure 4: (**A**) Rapamycin treatment decreased the level of phosphorylated mTOR (*$p<0.05$), but were unchanged with U18666A treatment and cholesterol depletion. (**B**) Up-regulation of beclin-1 levels was not observed with any of the three treatments. The results are expressed as a ratio relative to those from corresponding untreated controls at each time point. Data shows mean ± SD from four independent experiments. (**C**) 6 hour treatment with 100 nM wortmannin surpressed amino-acid-starvation-induced autophagy. (**D, E**) 6 hour treatment with wortmannin did not affect the levels of LC3-11 and A*β*

activity[30]. However, autophagy is a dynamic, multistep process that can be modulated at several levels, and therefore, static measurements do not reflect the precise time course of autophagic activity[31–33]. Moreover, it is recognized that LC3 protein tends to aggregate independently of autophagic activity. LC3 protein can be transiently overexpressed or intracellular protein aggregates form even in autophagy-deficient cell lines[34]. Therefore, recent guidelines for the use and interpretation for monitoring autophagy in higher eukaryotes have recommended the use of multiple assays to verify the presence of an autophagic response. It is essential to distinguish between autophagosomes or LC3-II accumulation and autophagic flux. We showed changes in autophagosomes both from the increase in LC3-positive structures and from the elevation of the level of LC3-II under all three experimental conditions, rapamycin, U18666A treatments and cholesterol depletion. However, their effects on secreted and intracellular Aβ differed.

One explanation for the discrepancy in our results is that although each treatment caused an increase in autophagic activity, differences in the activating pathways resulted in different effects on Aβ levels. Two major autophagic pathways have been proposed. One is based on mTOR dephosphorylation, the other on beclin-1 activation[35]. Both our results and previous reports[5] clearly show AV proliferation accompanied by a decrease in phosphorylated mTOR levels that resulted in an increase in secreted and intracellular Aβ, whereas the absence of changes in phosphorylated mTOR levels produced the opposite effects. However, beclin-1 levels were not related to the levels of Aβ. Pacheco *et al.*[20] reported that autophagy is dependent on beclin-1 rather than on mTOR in NPC. Although our results were not statistically significant, the beclin-1 level tended to increase in the U18666A-treated cells. The reason for our failure to observe changes in beclin-1 levels is unclear, but a contributing factor may be the variations in the degradative capacity in different cell lines. It is also relevant that the PI3K inhibitor, wortmannin, inhibited the elevation of LC3-II induced by conventional starvation, but did not inhibit the elevation caused by U18666A. The variations seen in Aβ generation and secretion may reflect differences in the underlying mechanisms in each of these three conditions.

The variations observed in Aβ generation may be due to the interpretation of increased LC3 signals; raised immunoreactivity does not inevitably reflect an increase in autophagic activity. Autophagy begins with the formation of double-membrane-bound autophagosomes. Subsequently, autophagosomes fuse with lysosomes to form autophagolysosomes, and the contents of the vesicles are finally broken down by acidic lysosomal hydrolases[33]. Increased numbers of autophagosomes are observed when AV maturation is blocked. It is reasonable to conclude that the observed increases in LC3 signals measured with immunoblotting and immunocytochemistry reflect the disruption of the degeneration process, especially at later stages[8,14,32]. The three treatments in all our experiments caused an increase in AVs. However, the results of our immunocytochemical study showed that the numbers, sizes and distributions of LC3-positive granules in the U18666A-treated and cholesterol-depleted cells were different from those in the rapamycin-treated cells. These results suggest that there is an increase in LC3-II levels in AV formation each of the different stages. It has been reported that the LC3-positive granules that aggregate and colocalize with cholesterol clusters in Purkinje cells in NPC1 knockout mice are different in size and distribution than those in normal LC3-positive autophagosomes, indicating an abnormal autophagy lysosome system[14]. Cheng *et al.*[32] has also described large autophagosomes in statin-cholesterol-depleted cells, suggesting an impairment of autophagosome–lysosome fusion, compared with those induced by amino acid starvation. Some of these large circular LC3-positive structures colocalized with the weak lysosomal-associated late endosome/lysosome marker membrane protein 1[25]. It is possible that the variations in morphological characteristics of the LC3-positive granules in our experiments reflect an impairment in the evolution of AVs, suggesting that secreted and intracellular Aβ are both affected by the steps in AV maturation.

A third explanation for our results may be that cholesterol depletion and U18666A treatment act on different Aβ generation and secretion sites. Lipid rafts have been proposed as one of the possible cellular Aβ production sites[36–38]. Lipid rafts are membrane-domains rich in cholesterol and sphingolipids[39,40], contain β-secretase (β-site APP-cleaving enzyme, BACE1), and can be internalized to endosomes[36,39,40]. BACE1 and APP coexist in endosomes, the possible preferential site of BACE1 activity due to its acidic pH[40]. U18666A suppresses the export of free cholesterol from late endosomes, resulting in a decrease in cholesterol in cell membranes[24]. Both cholesterol depletion and U18666A treatment decrease cholesterol content in lipid rafts, disrupting their formation and function[39,41,42]. Cholesterol is also known to be important for protein trafficking by lipid rafts[43]. These findings suggest that impaired function and trafficking in lipid rafts caused by U18666A treatment or cholesterol depletion could result in the production and secretion of Aβ. Because large amounts of Aβ were secreted from cells even when autophagy was inhibited and low numbers of AVs were detected in normal brain *in vivo*, it is possible that autophagy may play minor role in constitutive Aβ generation[5]. Cholesterol depletion and U18666A treatment may decrease Aβ production by affecting major generation sites even if the LC3 signals are augmented by increased autophagic activity or disruption of autophagosomal breakdown.

Yu *et al.*[5] described increases in both LC3-II levels and AV population (at EM level) and that the appearance of LC3 immunoreactive structures precedes Aβ deposition in both preclinical AD brains *in vivo* and in young PS1/APP mice ('predepositing' mice). These observations suggest that autophagy is induced at a very early age. These authors also described a robust accumulation of autophagosomes and autophagolysosomes during advanced

stages in AD and PS1/APP brains and concluded that their observations reflected strong autophagic activation or a failed maturation of autophagosomes to lysosomes or both[5]. They claimed that stimulation of AV production and delay or impairment in the maturation of AVs to lysosomes may cause an increase the number of AVs, with a subsequent rise in intracellular Aβ levels[5]. However, our experiments did not show a consistent rise in intracellular Aβ levels in cells with a similar increase in LC3 immunoreactivity. Reports of reduced beclin-1 levels in affected brain regions of patients with early AD suggest that disruption of neuronal autophagy occurs in AD[6]. It therefore appears that neuronal autophagy is important in AD pathology, but the precise role of autophagy in the disease process remains unclear.

ACKNOWLEDGEMENT

This study was supported by grants from the Ministry of Health, Labor and Welfare and the Ministry of Education, Culture, Sports, Science and Technology of Japan to K. Okamoto.

REFERENCES

1 Mattson MP. Pathways towards and away from Alzheimer's disease. *Nature* 2004; **430**: 631–639
2 Selkoe DJ, Schenk D. Alzheimer's disease: Molecular understanding predicts amyloid-based therapeutics. *Annu Rev Pharmacol Toxicol* 2003; **43**: 545–584
3 Cupers P, Bentahir M, Craessaerts K, *et al.* The discrepancy between presenilin subcellular localization and γ-secretase processing of amyloid precursor protein. *J Cell Biol* 2001; **154**: 731–740
4 Nixon RA, Wegiel J, Kumar A, *et al.* Extensive involvement of autophagy in Alzheimer disease: An immuno-electron microscopy study. *J Neuropathol Exp Neurol* 2005; **64**: 113–122
5 Yu WH, Cuervo AM, Kumar A, *et al.* Macroautophagy – a novel β-amyloid peptide-generating pathway activated in Alzheimer's disease. *J Cell Biol* 2005; **171**: 87–98
6 Pickford F, Masliah E, Britschgi M, *et al.* The autophagy related protein beclin 1 shows reduced expression in early Alzheimer disease and regulates amyloid β accumulation in mice. *J Clin Invest* 2008; **118**: 2190–2199
7 Mortimore GE, Pösö AR. Intracellular protein catabolism and its control during nutrient deprivation and supply. *Annu Rev Nutr* 1987; **7**: 539–564
8 Tanida I, Minematsu-Ikeguchi N, Ueno T, *et al.* Lysosomal turnover, but not a cellular level, of endogenous LC3 is a marker for autophagy. *Autophagy* 2005; **1**: 84–91
9 Koo EH, Squazzo SL. Evidence that production and release of amyloid β-protein involves the endocytic pathway. *J Biol Chem* 1994; **269**: 17386–17389
10 Ravikumar B, Duden R, Rubinsztein DC. Aggregate-prone proteins with polyglutamine and polyalanine expansions are degraded by autophagy. *Hum Mol Genet* 2002; **11**: 1107–1117
11 Yamazaki T, Chang TY, Haass C, *et al.* Accumulation and aggregation of amyloid β-protein in late endosomes of Niemann–Pick type C cells. *J Biol Chem* 2001; **276**: 4454–4460
12 Powis G, Bonjouklian R, Berggren MM, *et al.* Wortmannin, a potent and selective inhibitor of phosphatidylinositol-3-kinase. *Cancer Res* 1994; **54**: 2419–2423
13 Ui M, Okada T, Hazeki K, *et al.* Wortmannin as a unique probe for an intracellular signaling protein, phosphoinoside 3-kinase. *Trends Biochem Sci* 1995; **20**: 303–307
14 Kabeya Y, Mizushima N, Ueno T, *et al.* LC3, a mammalian homologue of yeast Apg8p, is localized in autophagosome membranes after processing. *EMBO J* 2000; **19**: 5720–5728
15 Yoshimori T, Semba T, Takemoto H, *et al.* Protein disulfide-isomerase in rat exocrine pancreatic cells is exported from the endoplasmic reticulum despite possessing the retention signal. *J Biol Chem* 1990; **265**: 15984–15990
16 Lu Z, Dono K, Gotoh K, *et al.* Participation of autophagy in the degeneration process of rat hepatocytes after transplantation following prolonged cold preservation. *Arch Histol Cytol* 2005; **68**: 71–80
17 McLean CA, Cherny RA, Fraser FW, *et al.* Soluble pool of Aβ amyloid as a determinant of severity of neurodegeneration in Alzheimer's disease. *Ann Neurol* 1999; **46**: 860–866
18 Ida N, Hartmann T, Pantel J, *et al.* Analysis of heterogeneous A4 peptides in human cerebrospinal fluid and blood by a newly developed sensitive Western blot assay. *J Biol Chem* 1996; **271**: 22908–22914
19 Liao G, Yao Y, Liu J, *et al.* Cholesterol accumulation is associated with lysosomal dysfunction and autophagic stress in Npc1 −/− mouse brain. *Am J Pathol* 2007; **171**: 962–975
20 Pacheco CD, Kunkel R, Lieberman AP. Autophagy in Niemann–Pick C disease is dependent upon Beclin-1 and responsive to lipid trafficking defects. *Hum Mol Genet* 2007; **16**: 1495–1503
21 Pentchev PG, Vanier MT, Suzuki K, *et al.* Niemann–Pick disease type C: Cellular cholesterol lipidosis. In: Scirver CR, Beaudet AL, Sly WS, *et al.*, eds. *The Metabolic and Molecular Basis of Inherited Disease*, New York: McGraw–Hill Inc, 1995: pp. 2625–2639
22 Kobayashi T, Beuchat MH, Lindsay M, *et al.* Late endosomal membranes rich in lysobisphosphatidic acid regulate cholesterol transport. *Nat Cell Biol* 1999; **1**: 113–118
23 Love S, Bridges LR, Case CP. Neurofibrillary tangles in Niemann–Pick disease type C. *Brain* 1995; **118**: 119–129
24 Lange Y, Steck TL. Cholesterol homeostasis. Modulation by amphiphiles. *J Biol Chem* 1994; **269**: 29371–29374
25 Cheng J, Ohsaki Y, Tauchi-Sato K, *et al.* Cholesterol depletion induces autophagy. *Biochem Biophys Res Commun* 2006; **351**: 246–252
26 Liscum L, Faust JR. The intracellular transport of low density lipoprotein-derived cholesterol is inhibited in Chinese hamster ovary cells cultured with 3-β-[2-(diethylamino)ethoxy]androst-5-en-17-one. *J Biol Chem* 1989; **264**: 11796–11806
27 Klionsky DJ, Emr SD. Autophagy as a regulated pathway of cellular degradation. *Science* 2000; **290**: 1717–1721
28 Brunn GJ, Williams J, Sabers C, *et al.* Direct inhibition of signaling function of the mammalian target of rapamycin by the phosphatidylinositide-3-kinase inhibitors, wortmannin and LY294002. *EMBO J* 1996; **15**: 5256–5267
29 Blommaart EF, Krause U, Schellens JP, *et al.* The phosphatidylinositol 3-kinase inhibitors wortmannin and LY2940002 inhibit autophagy in isolated rat hepatocytes. *Eur J Biochem* 1997; **243**: 240–246
30 Mizushima N, Yamamoto A, Matsui M, *et al.* In vivo analysis of autophagy in response to nutrient starvation using transgenic mice expressing a fluorescent autophagosome marker. *Mol Biol Cell* 2004; **15**: 1101–1111
31 Mizushima N, Klionsky DJ. Protein turnover via autophagy: Implications for metabolism. *Annu Rev Nutr* 2007; **27**: 19–39
32 Klionsky DJ, Abeliovich H, Agostinis P, *et al.* Guidelines for the use and interpretation of assays for monitoring autophagy in higher eukaryotes. *Autophagy* 2008; **4**: 151–75
33 Mizushima N, Ohsumi Y, Yoshimori T. Autophagosome formation in mammalian cells. *Cell Struct Funct* 2002; **27**: 421–429
34 Kuma A, Matsui M, Mizushima N. LC3, an autophagosome marker, can be incorporated into protein aggregates independent of autophagy. *Autophagy* 2007; **3**: 323–328
35 Kihara A, Kabeya Y, Ohsumi Y, *et al.* Beclin-phosphatidylinositol 3-kinase complex functions at the trans-Golgi network. *EMBO Rep* 2001; **2**: 330–335
36 Ehehalt R, Keller P, Haass C, *et al.* Amyloidogenic processing of the Alzheimer β-amyloid precursor protein depends on lipid raft. *J Cell Biol* 2003; **160**: 113–123
37 Kawarabayashi T, Shoji M, Younkin LH, *et al.* Dimeric amyloid β protein rapidly accumulates in lipid rafts followed by apolipoprotein E and phosphorylated tau accumulation in the Tg2576 mouse model of Alzheimer's disease. *J Neurosci* 2004; **24**: 3801–3809
38 Simons M, Keller P, De Strooper B, *et al.* Cholesterol depletion inhibits the generation of β-amyloid in hippocampal neurons. *Proc Natl Acad Sci USA* 1998; **95**: 6460–6464
39 Simons K, Toomre D. Lipid rafts and signal transduction. *Nat Rev Mol Cell Biol* 2000; **1**: 31–39

40 Haass C. Take five – BACE and the gamma-secretase quartet conduct Alzheimer's amyloid β-peptide generation. *EMBO J* 2004; **23**: 483–488
41 Hannan LA, Edidin M. Traffic, polarity, and detergent solubility of a glycosylphosphatidylinositol-anchored protein after LDL-deprivation of MDCK cells. *J Cell Biol* 1996; **133**: 1265–1276
42 Van der Luit AH, Budde M, Zerp S, *et al.* Resistance to alkyl-lysophospholipid-induced apoptosis due to downregulated sphingomyelin synthase 1 expression with consequent sphingomyelin- and cholesterol-deficiency in lipid rafts. *Biochem J* 2007; **401**: 541–549
43 Simons K, Ikonen E. Functional rafts in cell membranes. *Nature* 1997; **387**: 569–572